

May 17, 2022

TWS et al.
June 2022 Lease Sale Protests

EXHIBIT E

DOI-BLM-CO-0000-2022-0001-EA
DOI-BLM-MT-0000-2021-0006-EA
DOI-BLM-NM-P000-2021-0001-EA
DOI-BLM-NM-0040-2021-0033-EA
DOI-BLM-NV-B000-2021-0007-OTHER
DOI-BLM-UT-0000-2021-0007-EA
DOI-BLM-WY-0000-2021-0003-EA

LETTER • OPEN ACCESS

Up in smoke: characterizing the population exposed to flaring from unconventional oil and gas development in the contiguous US

To cite this article: Lara J Cushing *et al* 2021 *Environ. Res. Lett.* **16** 034032

View the [article online](#) for updates and enhancements.

You may also like

- [New Time-resolved, Multi-band Flares in the GJ 65 System with gPhoton](#)
Scott W. Fleming, Chase Million, Rachel A. Osten et al.
- [NIMBY, YIMBY, or something else? Geographies of public perceptions of shale gas development in the Marcellus Shale](#)
Chad Zanocco, Hilary Boudet, Christopher E Clarke et al.
- [THE YOUNG BINARY DQ Tau: A HUNT FOR X-RAY EMISSION FROM COLLIDING MAGNETOSPHERES](#)
Konstantin V. Getman, Patrick S. Broos, Demere M. Salter et al.

ENVIRONMENTAL RESEARCH
LETTERS

LETTER

OPEN ACCESS

RECEIVED
22 October 2020REVISED
1 December 2020ACCEPTED FOR PUBLICATION
15 December 2020PUBLISHED
23 February 2021

Original content from
this work may be used
under the terms of the
[Creative Commons
Attribution 4.0 licence](#).

Any further distribution
of this work must
maintain attribution to
the author(s) and the title
of the work, journal
citation and DOI.



Up in smoke: characterizing the population exposed to flaring from unconventional oil and gas development in the contiguous US

Lara J Cushing¹ , Khang Chau², Meredith Franklin² and Jill E Johnston²¹ Department Environmental Health Sciences, University of California, Los Angeles, CA, United States of America² Department of Preventive Medicine, University of Southern California, Los Angeles, CA, United States of AmericaE-mail: lcushing@ucla.edu and jillj@usc.edu**Keywords:** hydraulic fracturing, remote-sensing, dasymetric mapping, environmental justiceSupplementary material for this article is available [online](#)**Abstract**

Due to advances in unconventional extraction techniques, the rate of fossil fuel production in the United States (US) is higher than ever before. The disposal of waste gas via intentional combustion (flaring) from unconventional oil and gas (UOG) development has also been on the rise, and may expose nearby residents to toxic air pollutants, light pollution and noise. However, little data exists on the extent of flaring in the US or the number of people living near UOG flaring activity.

Utilizing nightly satellite observations of flaring from the Visible Infrared Imaging Radiometer Suite Nightfire product, 2010 Census data and a dataset of remotely sensed building footprints, we applied a dasymetric mapping approach to estimate the number of nightly flare events across all oil shale plays in the contiguous US between March 2012 and February 2020 and characterize the populations residing within 3 km, 5 km and 10 km of UOG flares in terms of age, race and ethnicity. We found that three basins accounted for over 83% of all UOG flaring activity in the contiguous US over the 8 year study period. We estimated that over half a million people in these basins reside within 5 km of a flare, and 39% of them lived near more than 100 nightly flares. Black, indigenous, and people of color were disproportionately exposed to flaring.

1. Introduction

With the rise of unconventional extraction techniques, domestic oil and gas production in the United States (US) has increased to its highest level on historical record. Oil production has more than doubled since 2010, reversing a longstanding decline in production, while natural gas withdrawals have risen by 60% (U.S. Energy Information Administration 2020a, 2020b). This has been made possible in large part by advancements in directional drilling and high volume hydraulic fracturing ('fracking'), which involves the injection of fluids, sands, and chemical additives into wells (Colborn *et al* 2011, Webb *et al* 2014, Kassotis *et al* 2016). These unconventional extraction techniques have allowed for the development of oil and gas from areas that were previously inaccessible or uneconomical. An estimated 17.6 million residents of the contiguous US now live less than 1 mile from an active oil or gas well, raising concerns

about the potential for harmful environmental exposures and impacts on public health (Czolowski *et al* 2017). Unconventional oil and gas (UOG) drilling has been linked to worsened air quality (Field *et al* 2014, Macey *et al* 2014, Garcia-Gonzales *et al* 2019), contaminated water (Schmidt 2013, Elliott *et al* 2017), increased noise (Blair *et al* 2018, Allshouse *et al* 2019), more traffic (Adgate *et al* 2014), and disruptions to the local social fabric (Witter *et al* 2013). There is also growing evidence linking UOG operations with negative health impacts for nearby residents, including impacts on fetal growth and preterm birth (McKenzie *et al* 2014, Casey *et al* 2015, Stacy *et al* 2015, Whitworth *et al* 2018, Gonzalez *et al* 2020, Tran *et al* 2020).

One consequence of the rapid expansion of fossil fuel extraction is flaring, the practice of intentionally combusting excess natural gas to the open atmosphere. Flaring is used during the exploration, production and processing of fossil fuels and is common in oil-producing shale plays with insufficient

infrastructure for the capture and utilization of natural gas that is recovered with the oil. Shale plays are accumulations of oil and natural gas deposits within fine-grained sedimentary rock and are located within large-scale geologic depressions called basins. Air quality monitoring studies indicate that flares—which often operate continuously for days or weeks (Johnson and Coderre 2011)—release a variety of hazardous air pollutants including volatile organic compounds and polycyclic aromatic hydrocarbons along with carbon monoxide, nitrogen oxides (NO_x), and black carbon (Stroscher 1996, Kindzierski 1999, Leahey *et al* 2001, Ite and Ibok 2013, Fawole *et al* 2016, Gvakharia *et al* 2017, Schade and Roest 2018, Giwa *et al* 2019, Roest and Schade 2020). In recent years, flaring in the US grew substantially, and the US was responsible for the highest number of flares of any country globally, with an estimated 17.3 billion m³ of natural gas flared in 2019 (Elvidge *et al* 2015, World Bank 2020). This represents a 23% increase from the prior year (World Bank 2020). However, because the practice is largely unregulated, information on flaring from UOG varies by state and is often limited to aggregate (e.g. monthly, field-level) data self-reported by industry operators. A recent analysis in Texas suggests that flaring volumes reported to state regulators represent about one half of actual flare activity, highlighting the limitations of state regulatory data to assess gas flaring activity (Willyard and Schade 2019). The lack of detailed and objective information on the location of flaring from UOG also means that the number of people residing in close proximity to UOG flaring who could be exposed to flaring-related air pollutants is poorly characterized.

In prior work we used satellite observations to measure flaring activity in the Eagle Ford Shale of South Texas (Franklin *et al* 2019, Johnston *et al* 2020), and found that exposure to significant levels of flaring during pregnancy was associated with increased risk of preterm birth among women living within 5 km of flares (Cushing *et al* 2020). Here, we extend our approach to quantify the amount of flaring across the contiguous US over the last eight years and provide the first nationwide estimate of the number of people living near UOG flaring. We utilize a dasymetric mapping approach to estimate the exposed population. Dasymetric mapping refers to the process of disaggregating spatial data to a finer spatial unit of analysis using ancillary data (Mennis 2003). The smallest spatial unit for population data from the US Census Bureau is ‘census blocks’. In cities, census blocks generally correspond to city blocks. However, flaring occurs primarily in rural areas where census blocks can encompass hundreds of square miles and very few people. We utilize a remotely sensed dataset of building footprints to decompose block-level population counts to the finer spatial unit of analysis of buildings and more accurately estimate the number of people living near UOG flaring.

2. Methods

2.1. Study area

We utilized data from the U.S. Energy Information Administration (EIA) to define the boundaries of all oil and gas shale plays in the contiguous US (n.d.). This data was updated in 2016 and includes 47 shale plays within 28 basins that intersect 714 counties across 28 states. We first estimated the density of nightly flares (count per square km) across all 28 basins, and then narrowed our study area and further refined our estimates in the three basins with the most flaring activity: the Permian, Western Gulf (Eagle Ford Shale), and Williston (Bakken shale). These three basins cover 86 counties in 4 states: 31 counties in the Permian (4 in New Mexico and 27 in Texas), 25 in the Western Gulf (Texas), and 30 in Williston (8 in Montana and 22 in North Dakota).

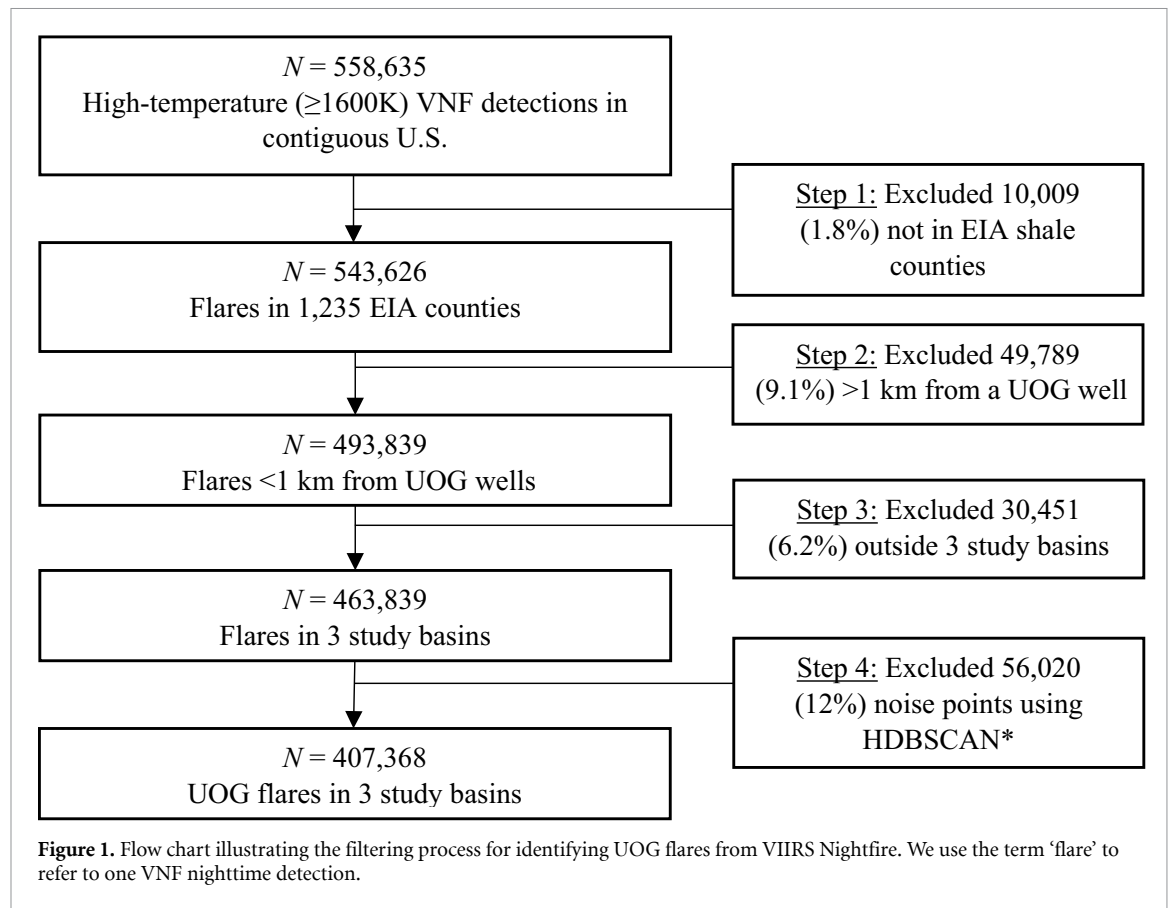
2.2. UOG wells

We obtained data on UOG wells for the entire contiguous US from Enverus (www.enverus.com, formerly DrillingInfo). The data include well locations (latitude and longitude), various attributes such as drill type (horizontal or directional), production type (oil or gas), production volumes (in barrels [BBL] oil or in thousands of cubic feet of gas [MCF]—which we converted to barrels of oil equivalent [BOE = MCF/6]). We restricted the data to horizontal- and directional-drilled wells that were actively producing during our study period: March 2012 through February 2020.

2.3. VIIRS Nightfire

Flares were identified using the Visible Infrared Imaging Radiometer Suite (VIIRS) instrument Nightfire (VNF) product from the National Oceanic and Atmospheric Administration Earth Observation Group. The VNF algorithm uses near-infrared and short-wave infrared bands to detect locations of nighttime subpixel (<750 m) combustion sources (Elvidge *et al* 2013). For each detected ‘hotspot’, the VNF product provides information on source temperature, area, and radiant heat. VIIRS began collecting data in March 2012; hence, March 2012 is the first month of our 8 year study period.

We filtered the VNF data in order to limit our sample to observations that were associated with UOG extraction (figure 1). First, a black-body temperature threshold of 1600 K was used to distinguish likely UOG-related flares from other sources of combustion such as biomass burning. Prior work shows VNF detections exhibit a bimodal temperature distribution, with detections related to biomass burning primarily observed between 800 and 1200 K, and the bulk of flaring-associated detections being between 1700 and 1800 K (Elvidge *et al* 2013). We chose the



1600 K cut off to be conservative, because 1300–1500 K is a cross over range where detections may result from both biomass burning and flaring (Elvidge *et al* 2015). Second, we restricted our sample to VNF detections within 1 km of actively producing UOG wells in order to reduce the likelihood of including observations unrelated to UOG production, such as flaring at refineries. We then estimated the density of the resulting set of VNF detections across all 714 counties in the 28 EIA-defined basins at 10×10 km resolution with a Gaussian kernel density function. Finally, we utilized Hierarchical Density-Based Spatial Clustering Application with Noise (HDBSCAN*) to remove possible aberrant observations as described in detail elsewhere (Franklin *et al* 2019). Because of the computational intensity involved and scarcity of flaring in other basins, HDBSCAN* was performed only for the three basins with the greatest density of flares. The 86 counties in these three basins accounted for 94% of the high-temperature VNF detections near wells identified in the previous step (figure 1).

HDBSCAN* is an unsupervised clustering method that requires only one input parameter—the minimum number of points required in a cluster, k —and does not require setting the number of clusters *a priori* as with other clustering methods (e.g. K -means clustering). Using a minimum spanning tree that connects every point in the sample and calculating cluster-stability scores, the algorithm identifies k -minimum clusters and noise points that do not

belong to any cluster. In previous work on UOG-related flaring in the Eagle Ford Shale, we applied HDBSCAN* and observed that clustered VNF detections were closer on average to active UOG wells compared to noise detections (Franklin *et al* 2019). We extended the same approach here: for each basin, we used HDBSCAN* to identify clusters of VNF detections and excluded detections classified as noise. The clustering process involves tuning for the best k —resulting in the fewest number of noise points identified—for each basin and for each year. Flares detected in January and February 2020 were combined with flares from 2019 for the clustering process. Hereafter, we refer to our final sample of $N = 407\,368$ high-temperature (>1600 K), HDBSCAN*-clustered VNF detections near wells as ‘UOG flares’. We therefore use the term flare to refer to one nighttime VNF detection.

2.4. Population and demographic data

We obtained demographic data from the National Historical Geographic Information System (Manson *et al* 2018). We utilized 2010 U.S. Census data to identify populations living near flaring and assess their demographic characteristics at the smallest census geography available—the census block. While more recent population estimates are available from the American Community Survey, they are based on a sample and thus less accurate and are only available at more aggregated geographies (census block

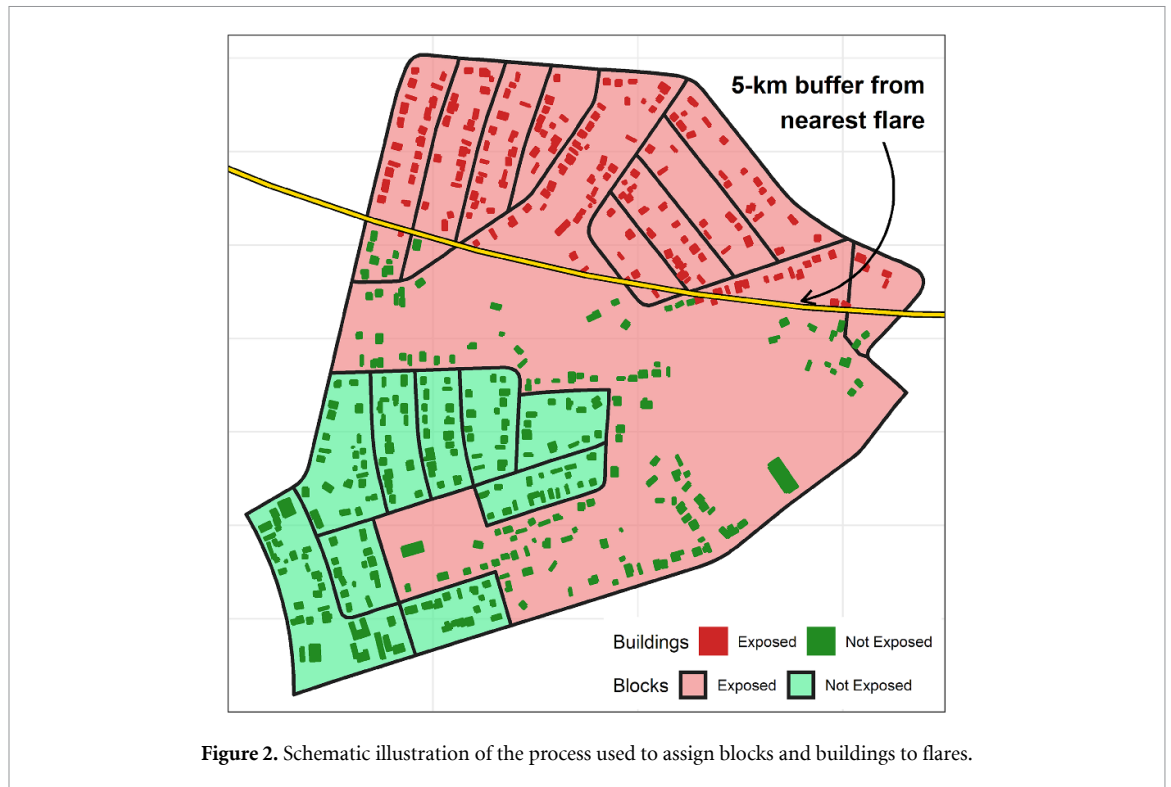


Figure 2. Schematic illustration of the process used to assign blocks and buildings to flares.

groups, which can be very large in our largely rural study areas). We examined population demographics by age (<5 and 65 or older) and race/ethnicity (Hispanic of any race, non-Hispanic White, non-Hispanic Black, non-Hispanic Native American, and all other non-Hispanic groups, including mixed race). Some racial and ethnic groups were collapsed due to the low number of individuals. We also obtained county-level population data from the 2018 American Community Survey to evaluate changes in population since 2010.

2.5. Building footprints

Because census blocks can be large in rural areas, we conducted dasymetric mapping using a national dataset of building footprints generated by Microsoft to refine our exposure assessment, illustrated in figure 2 (Anon 2019). Dasymetric mapping refers to the process of disaggregating spatial data—in this case 2010 census blocks—to a finer spatial unit of analysis using ancillary data (Mennis 2003), and has been used in previous studies of exposure to UOG development (Clough and Bell 2016). The Microsoft Building Footprint data were created using a two-stage process in which deep neural networks were used on satellite imagery to identify building pixels (semantic segmentation), and these aggregations of building pixels were then converted into polygons across all 50 US states. In our 86 counties of primary interest, we identified all buildings whose centroids fell within census blocks with non-zero populations. For a given block, we assigned population counts to those build-

ings by assuming a uniform distribution of total, age-specific, and race/ethnicity-specific populations within the block. This resulted in fractions of persons at the building level that we then summed to generate more refined population estimates at the levels of counties, states and basins. While an improvement over traditional methods relying on census block geography, our approach makes the simplifying assumptions that (a) all buildings are residential (as opposed to being commercial or other types of uninhabited buildings) and (b) the population within each census block is uniformly distributed with respect to age and race/ethnicity. A small number of blocks with non-zero populations contained no buildings (<3% of blocks and 1% of people in our study area). In these cases, those populations were not assigned to any building or included in our dasymetric mapping-based estimates.

For each block and building, we counted the number of UOG flares that fell within its 5 km circular buffer. We focused on the 5 km distance given our prior finding of adverse associations between flaring and preterm birth at this distance (Cushing *et al* 2020); however, we also considered 3 km and 10 km buffers since studies of flaring are limited and the distance at which flares may result in potentially harmful exposures to nearby populations is not well understood. At the basin level, we compared our estimates of the number and demographics of people exposed derived from the dasymetric mapping with building footprints to the estimates that resulted from using census blocks alone.

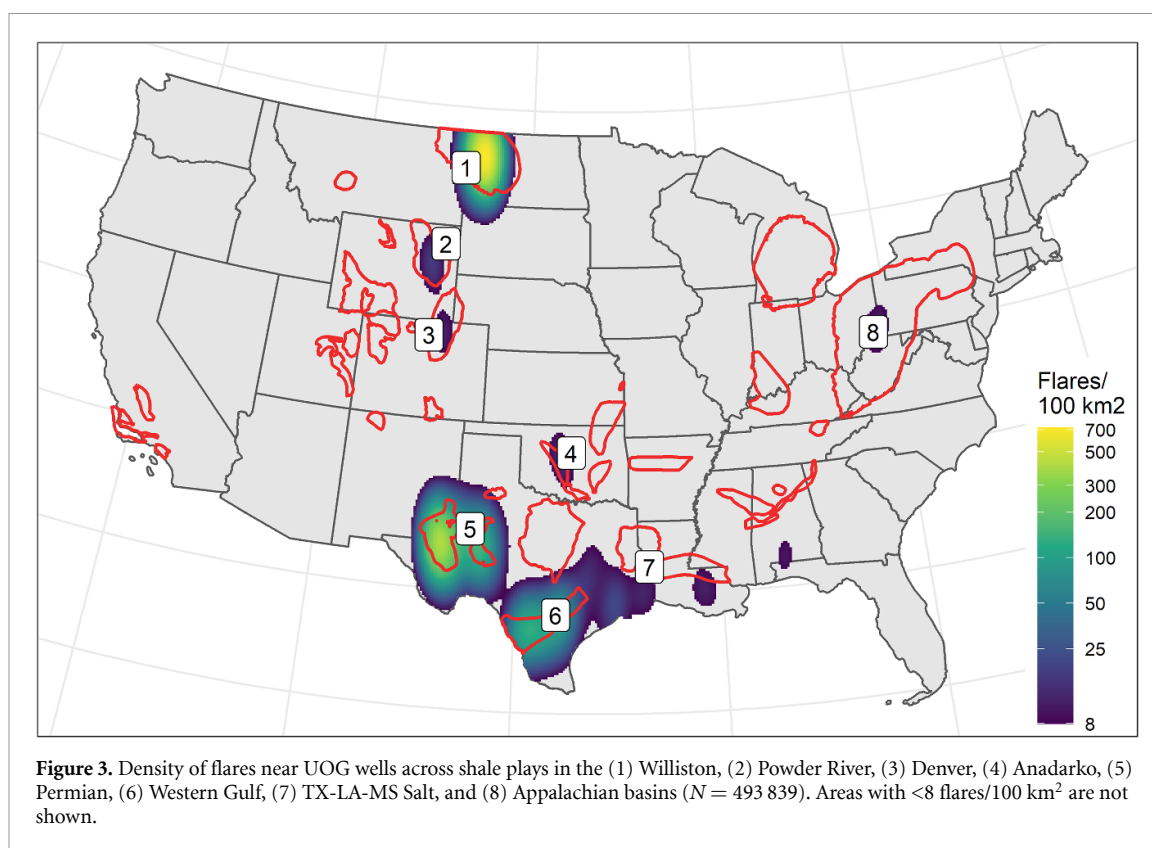


Table 1. Basins with the at least 1000 UOG-related flares during the study period (March 2012–February 2020).

Basin	Flares ^a	Cumulative (%) ^b
Williston	195 497	195 497 (35.0)
Permian	191 989	387 486 (69.4)
Western Gulf	75 902	463 388 (83.0)
Appalachian	5039	468 427 (83.9)
Powder River	4852	473 279 (84.7)
Denver	3916	477 195 (85.4)
Anadarko	3608	480 803 (86.1)
TX-LA-MS Salt	1118	481 921 (86.3)

^a Count of high-temperature (≥ 1600 K) VNF detections within 1 km of a UOG well.

^b Percentage of all high-temperature VNF detections within the contiguous US.

3. Results

Eight basins contained a non-negligible number of flares (at least 1000 high-temperature VNF observations within 1 km from an active UOG well over the 8 year study period) (figure 3). The Williston, Permian, and Western Gulf basins that were the focus of our subsequent analysis accounted for 83% of all high-temperature (≥ 1600 K) VNF observations in the contiguous US (table 1). The Appalachian basin, whose shale plays cover a larger geographic area than those in the three basins combined, only included about 5000 ($<1\%$) UOG-related flares over the study period.

After further restricting to non-aberrant observations using HDBSCAN*, our final sample

across the Williston, Permian, and Western Gulf basins included 407 368 UOG flares. The total number of flares was highest in the Permian Basin (170 962), followed by Williston (167 235 flares) and Western Gulf (69 171 flares). The highest flare densities were observed in the Williston Basin (maximum of 716 (km²)⁻¹), followed by the Permian (413 (km²)⁻¹) and the Western Gulf (131 (km²)⁻¹) (figure S1 (available online at stacks.iop.org/ERL/16/034032/mmedia)). The top ten counties with the highest number of flares included four in Williston (McKenzie, Williams, Dunn, and Mountrail, North Dakota), four in the Permian (Reeves and Loving, Texas; and Eddy and Lea, New Mexico), and two in the Western Gulf (La Salle and Karnes, Texas) (table S1). No UOG flares were observed in 21 out of the 87 counties in these three basins. Overall, the number of flares in all three basins grew over time, particularly since 2018 (figure S2).

During the study period, there were approximately 31 000 actively producing UOG wells in the Permian Basin, 28 000 in the Western Gulf basin, and 18 000 in the Williston Basin. The Permian Basin was the most productive (4.5 billion BBL in oil production and 2.5 billion BOE in gas production) followed by the Western Gulf (3.5 billion BBL in oil and 2.8 billion BOE in gas). Although the Williston Basin experienced a similar number of UOG flares as the Permian Basin, only 3.25 billion BBL in oil and 0.85 billion BOE in gas were produced over the same period in Williston (figure 4). At the county level, the

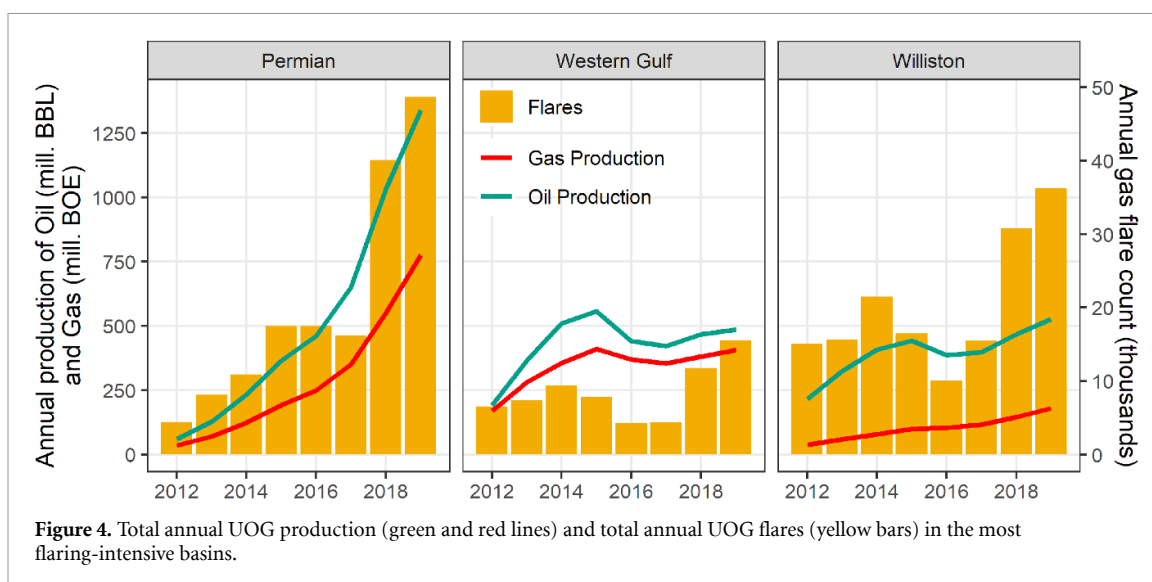


Figure 4. Total annual UOG production (green and red lines) and total annual UOG flares (yellow bars) in the most flaring-intensive basins.

Table 2. Population living within 5 km of UOG flares by basin, age group, and race/ethnicity.

Basin	Group ^a	Total N	Population exposed N (%)			
			Any flares	1–9 flares	10–99 flares	100+ flares ^b
Permian	All	783 688	358 167 (45.7)	98 469 (12.6)	115 998 (14.8)	143 700 (18.3)
	Age <5	62 263	29 158 (46.8)	8492 (13.6)	9135 (14.7)	11 531 (18.5)
	Age 65+	95 582	40 591 (42.5)	10 481 (11.0)	13 701 (14.3)	16 409 (17.2)
	Hispanic	356 697	160 662 (45.0)	46 189 (12.9)	48 134 (13.5)	66 339 (18.6)
	White	379 337	172 367 (45.4)	46 312 (12.2)	60 416 (15.9)	65 639 (17.3)
	Black	29 527	16 717 (56.6)	3754 (12.7)	4679 (15.8)	8284 (28.1)
	Native	3954	1797 (45.4)	579 (14.6)	623 (15.8)	595 (15.0)
	Others	14 173	6623 (46.7)	1634 (11.5)	2146 (15.1)	2843 (20.1)
	All	949 511	113 253 (11.9)	38 399 (4.0)	42 134 (4.4)	32 720 (3.5)
Western Gulf	Age <5	72 262	7141 (9.9)	2399 (3.3)	2628 (3.6)	2114 (2.9)
	Age 65+	116 284	18 662 (16.1)	6298 (5.4)	6361 (5.5)	6003 (5.2)
	Hispanic	549 970	49 365 (9.0)	16 243 (3.0)	19 388 (3.5)	13 734 (2.5)
	White	340 301	55 042 (16.2)	18 810 (5.5)	18 937 (5.6)	17 295 (5.1)
	Black	43 198	7478 (17.3)	2856 (6.6)	3287 (7.6)	1335 (3.1)
	Native	2412	273 (11.3)	92 (3.8)	100 (4.1)	81 (3.4)
	Others	13 630	1094 (8.0)	397 (2.9)	422 (3.1)	275 (2.0)
	All	327 789	64 487 (19.7)	17 206 (5.3)	12 951 (4.0)	34 330 (10.5)
	Age <5	21 986	4326 (19.7)	1042 (4.7)	830 (3.8)	2454 (11.2)
Williston	Age 65+	50 431	10 059 (20.0)	3064 (6.1)	2033 (4.0)	4962 (9.8)
	Hispanic	6062	1485 (24.5)	372 (6.1)	394 (6.5)	719 (11.9)
	White	292 565	56 082 (19.2)	16 027 (5.5)	11 552 (3.9)	28 503 (9.7)
	Black	2495	231 (9.3)	145 (5.8)	15 (0.6)	71 (2.8)
	Native	19 341	5068 (26.2)	214 (1.1)	740 (3.8)	4114 (21.3)
	Others	7326	1621 (22.1)	448 (6.1)	249 (3.4)	924 (12.6)
	All	2 060 988	535 907 (26.0)	154 074 (7.5)	171 083 (8.3)	210 750 (10.2)

^a Hispanic includes all Hispanics regardless of race. White, Black, Native, and Other categories exclude those identifying as Hispanic.

^b The highest number of UOG flares exposed per block is 2166 in the Permian, 3065 in the Western Gulf, and 6387 in Williston.

number of UOG flares was more highly correlated with the volume of oil produced (Spearman correlation coefficient $r = 0.94$) than the volume of gas produced ($r = 0.86$) in the 8 year period.

We connected each UOG flare to the nearest well to identify the most likely production type (oil or gas) associated with each flare. In all three basins, most flares were attributed to oil-producing wells: 73% of flares in the Permian, 85% in the Western Gulf, and 99% in Williston. Aggregating the number of flares by the likely production source, we estimated 27 flares

per million BBL of oil and 18 flares per million BOE of gas produced in Permian, 17 flares per million BBL of oil and 4 flares per million BOE of gas produced in Western Gulf, and 51 flares per million BBL of oil and 2 flares per million BOE of gas produced in Williston.

Using the dasymetric mapping approach, we estimated that 535 907 people lived within 5 km of a UOG flare across the three basins (table 2). Relying on census blocks rather than dasymetric mapping resulted in 4%–13% larger estimates of the exposed population, depending on the basin (table S2). This

was most pronounced in the Western Gulf basin and when considering the smaller 3 km buffer distance. In terms of the intensity of exposure, more people in the Permian Basin lived within 5 km of over 100 flares than in any other basin. More than half of these were in Midland and Ector counties, which contain the cities of Midland and Odessa (data not shown).

In the Permian Basin, the proportion of children under five living near flares was slightly higher than the overall population, while in the Western Gulf, a higher proportion of seniors were exposed (table 2). With respect to race and ethnicity, Blacks were more likely to live within 5 km of a flare in the Permian Basin and Western Gulf than other groups. In the Williston, the Native American and Hispanic populations were the most likely to live near flares. In particular, over a fifth of the Native American population in Williston shale counties lived within 5 km of over 100 flares. Flaring is particularly intense in the Fort Berthold Reservation in North Dakota, which accounted for 70% of the Native American population exposed to more than 100 flares. McKenzie county, which includes part of the Fort Berthold Reservation, had the most UOG flares of any county nationally (83 000) and we estimated that virtually all (93%) of its 6400 residents lived within 5 km of more than 100 flares. Patterns with respect to age and race/ethnicity were consistent when we considered populations within 3 km or 10 km of flares (tables S3 and S4).

4. Discussion

In this comprehensive assessment, we estimated that three oil and gas producing regions accounted for over 80% of all UOG flaring activity in the contiguous US over the 8 year study period (March 2012–February 2020). The Permian Basin in West Texas and Eastern New Mexico accounted for the greatest number of individual nightly flares, while the flaring intensity of oil production was highest in the Williston Basin (Bakken Shale) in North Dakota and Montana. We estimate that over 535 000 people live within 5 km of flaring in these three regions, and among these, over 210 000 live within 5 km of 100 or more individual nightly flare events.

Although health studies of flaring are limited, residence within 5 km of ten or more flares during pregnancy was associated with a substantial and statistically significant increase in preterm birth in our prior work (Cushing *et al* 2020). In addition, monitoring studies from the Eagle Ford Shale indicate that flaring is a significant source of NO_x as well as more reactive compounds including formaldehyde, acetaldehyde and ethene (Schade and Roest 2018). Increasing atmospheric NO_x concentrations over the Bakken shale and Permian Basin have also been attributed to flaring (Duncan *et al* 2016). Nitrogen oxides contribute to the development and exacerbation of asthma

as well as the formation of ground-level ozone, which in turn is linked with effects on the respiratory, cardiovascular, and nervous systems and with reproductive effects and mortality (U.S. Environmental Protection Agency 2016, 2020). Lab-based investigations and field studies from North Dakota, the Niger Delta, and Alberta, Canada have moreover shown that flaring emits hydrocarbons—including benzene and polycyclic aromatic hydrocarbons (PAHs)—as well as particulate matter in the form of black carbon (Stroscher 1996, Ana *et al* 2012, Mcewen and Johnson 2012, Fawole *et al* 2016, Weyant *et al* 2016, Gvakharia *et al* 2017). Benzene and some PAHs are well established carcinogens (Agency for Toxic Substances and Disease Registry 1995, Agency for Toxic Substances Control Registry 2007, Kim *et al* 2013) and have also been linked to birth defects (Lupo *et al* 2011, 2012). Exposure to black carbon is associated with higher rates of all-cause and cardiovascular mortality as well as cardiopulmonary hospital admissions (Janssen *et al* 2011, 2012).

Together, this evidence indicates that a substantial number of people in the US could be at risk of health-damaging exposures due to flaring from UOG. However, the lack of routine air quality monitoring in these rural areas or systematic regulation and reporting of flaring activity limits efforts to estimate potential flaring-related exposures and associated health risks. Gaps in our knowledge remain about the characteristics of flaring-related emissions and contributions to local air quality in real-world settings, which are influenced by factors such as the composition of the waste gas, type and operating conditions of the flare and the resulting completeness of combustion, and local meteorology. Additional gaps remain with respect to the potential health impacts of flaring through pathways unrelated to air pollution such as noise and psychosocial stress. Flaring operations produce heat and noise (Abdulkareem and Odigure 2006, Nwoye *et al* 2014), and evidence suggests noise pollution in other contexts may have effects on cognition, mental health, wellbeing, and quality of life (Clark *et al* 2020). In an online survey, residents of the Permian Basin indicated increased distress in response to UOG-related environmental degradation (Elser *et al* 2020). Psychosocial stress has been linked to adverse health outcomes including hypertension and cardiovascular disease, and can exacerbate the effects of air pollutant and other chemical exposures (Clougherty *et al* 2010, Vesterinen *et al* 2017).

Our findings also show that flaring is an environmental justice issue. Flaring in the Williston Basin disproportionately impacts Native Americans, particularly members of the Mandan, Hidatsa, and Arikara Nation living on the Fort Berthold Indian Reservation. In the Permian and Western Gulf (Eagle Ford) basins, the majority of the population are people of color (table 2). These rural regions are also among some of the poorest in Texas (Tunstall 2015). While

we did not assess this in the current study, our prior work also showed that majority Hispanic census blocks in the Eagle Ford Shale had a higher number of flares within 5 km on average than less Hispanic census blocks (Johnston *et al* 2020). In general, rural US populations like those in our study areas face additional challenges to health such as poverty and lack of access to health care that contribute to an urban-rural gap in life expectancy that is widening and more severe for people of color (Singh and Siahpush 2014, James and Cossman 2017, Long *et al* 2018). Indigenous leaders have also highlighted the detrimental social and cultural impacts of the Bakken oil boom in native communities (Horwitz 2014, Finn *et al* 2017). Our findings reflect larger patterns of urban-rural exploitation in which resources like fossil fuels are extracted from rural areas for the primary benefit of urban populations (Kelly-Reif and Wing 2016). This ultimately undermines progress toward more sustainable systems of energy provision because, with a few exceptions such as Los Angeles, California, the urban majority do not experience the environmental and health consequences of oil and gas extraction.

Finally, flaring also holds implications for climate change. Flaring emits greenhouse gases including carbon dioxide and nitrogen oxides and is an important source of black carbon in the Arctic, where it contributes to radiative forcing (Stohl *et al* 2013). Recent global estimates suggest 150 billion cubic meters of gas are flared annually, equivalent to the total annual gas consumption of Sub-Saharan Africa (World Bank 2020). Flaring thus accounts for significant losses of recovered natural gas, further contributing to the carbon footprint and climate impact of the fossil fuel industry.

Strengths of our study include the use of objective satellite observations to identify flaring and asymmetric mapping to refine population estimates. While the VFN satellite data does not provide an estimate of the volume of gas flared, it does include information on flaring at much higher spatial and temporal resolution than regulatory data and does not rely on un-audited self reports by the industry. Utilizing building footprints rather than census blocks to estimate populations near flaring overall resulted in a more conservative and likely more accurate estimate of the exposed population. Of the three study regions, we observed the greatest difference in the size of the exposed population when using building footprints rather than census blocks in the Western Gulf (Eagle Ford Shale). This may be because the Western Gulf encompasses more urban areas than the other two basins, including the cities of Laredo and Eagle Pass; utilizing building footprints rather than census blocks resulted in the exclusion of more people from these more densely populated areas.

The building footprints data we used is however also subject to error associated with the algorithmic

classification of satellite imagery that introduces uncertainty into our estimates. We also did not have information on building usage (e.g. residential vs commercial) and may have assigned some populations to non-residential buildings. The date of the satellite imagery underlying the Microsoft Building Footprints dataset is also unknown, may vary across the study area, and may fail to capture new housing developments.

Our analysis likely underestimates the exposed population because we rely on the 2010 US Census data (the most recent available) and many oil producing regions have experienced population growth since then. For example, the 2018 American Community Survey suggests the population of McKenzie County, ND has doubled since 2010, likely due to the oil boom. Overall the population of our three study basins has increased between 8% and 17% between 2010 and 2018 (table S3). If the population growth followed a similar pattern to what we observed in 2010 with respect to the fraction of the population in each basin residing within 5 km of any flare, we have underestimated the exposed population by roughly 55 000 people.

5. Conclusions

Over half a million people in the US live within 5 km of flaring from oil and gas development. Given the recent increase in flaring and suggestive evidence of adverse health impacts to nearby residents, additional research and greater regulatory oversight of flaring is needed.

Data availability statement

The data that support the findings of this study are available upon reasonable request from the authors.

Acknowledgments

This work was supported by a grant from the National Institutes of Health/National Institute of Environmental Health Sciences (R21-ES028417).

ORCID iD

Lara J Cushing  <https://orcid.org/0000-0003-0640-6450>

References

- Abdulkareem A S and Odigure J O 2006 Deterministic model for noise dispersion from gas flaring: a case study of Niger—Delta area of Nigeria *Chem. Biochem. Eng. Q.* **20** 157–64
- Adgate J L, Goldstein B D and McKenzie L M 2014 Potential public health hazards, exposures and health effects from unconventional natural gas development *Environ. Sci. Technol.* **48** 8307–20

- Agency for Toxic Substances and Disease Registry 1995 Toxicological Profile for Polycyclic Aromatic Hydrocarbons (Atlanta, GA: Agency for Toxic Substances and Disease Registry) (<https://www.atsdr.cdc.gov/toxprofiles/tp69.pdf>)
- Agency for Toxic Substances Control Registry 2007 Toxicological Profile for Benzene (Atlanta, GA: Agency for Toxic Substances Control Registry) (www.atsdr.cdc.gov/ToxProfiles/tp3.pdf)
- Allshouse W B, Mckenzie L M, Barton K, Brindley S and Adgate J L 2019 Community noise and air pollution exposure during the development of a multi-well oil and gas pad *Environ. Sci. Technol.* **53** 7126–35
- Ana G R E E, Sridhar M K C and Emerole G O 2012 Polycyclic aromatic hydrocarbon burden in ambient air in selected Niger Delta communities in Nigeria *J. Air Waste Manage. Assoc.* **62** 18–25
- Anon 2019 Microsoft/USBuildingFootprints (Microsoft) (available at: <https://github.com/microsoft/USBuildingFootprints>)
- Blair B D, Brindley S, Dinkeloo E, Mckenzie L M and Adgate J L 2018 Residential noise from nearby oil and gas well construction and drilling *J. Expo. Sci. Environ. Epidemiol.* **28** 538–47
- Casey J A, Kim B F, Larsen J, Price L B and Nachman K E 2015 Industrial food animal production and community health *Curr. Environ. Health Rep.* **2** 259–71
- Clark C, Crumpler C and Notley H 2020 Evidence for environmental noise effects on health for the United Kingdom policy context: a systematic review of the effects of environmental noise on mental health, wellbeing, quality of life, cancer, dementia, birth, reproductive outcomes, and cognition *Int. J. Environ. Res. Public Health* **17** 393
- Clough E and Bell D 2016 Just fracking: a distributive environmental justice analysis of unconventional gas development in Pennsylvania, USA *Environ. Res. Lett.* **11** 025001
- Clougherty J E, Rossi C A, Lawrence J, Long M S, Diaz E A, Lim R H, McEwen B, Koutrakis P and Godleski J J 2010 Chronic social stress and susceptibility to concentrated ambient fine particles in rats *Environ. Health Perspect.* **118** 769–75
- Colborn T, Kwiatkowski C, Schultz K and Bachran M 2011 Natural gas operations from a public health perspective *Hum. Ecol. Risk Assess.: Int. J.* **17** 1039–56
- Cushing L J, Vavra-Musser K, Chau K, Franklin M and Johnston J E 2020 Flaring from unconventional oil and gas development and birth outcomes in the Eagle Ford Shale in South Texas *Environ. Health Perspect.* **128** 077003
- Czolowski E D, Santoro R L, Srebotnjak T and Shonkoff S B C 2017 Toward consistent methodology to quantify populations in proximity to oil and gas development: a national spatial analysis and review *Environ. Health Perspect.* **125** 086004
- Duncan B N, Lamsal L N, Thompson A M, Yoshida Y, Lu Z, Streets D G, Hurwitz M M and Pickering K E 2016 A space-based, high-resolution view of notable changes in urban NO_x pollution around the world (2005–2014) *J. Geophys. Res.* **121** 976–96
- Elliott E G, Ettinger A S, Leaderer B P, Bracken M B and Deziel N C 2017 A systematic evaluation of chemicals in hydraulic-fracturing fluids and wastewater for reproductive and developmental toxicity *J. Expos. Sci. Environ. Epidemiol.* **27** 90–99
- Elser H, Goldman-Mellor S, Morello-Frosch R, Deziel N C, Ranjbar K and Casey J A 2020 Petro-riskscape and environmental distress in West Texas: community perceptions of environmental degradation, threats, and loss *Energy Res. Soc. Sci.* **70** 101798
- Elvidge C D, Zhizhin M, Baugh K, Hsu F-C and Ghosh T 2015 Methods for global survey of natural gas flaring from visible infrared imaging radiometer suite data *Energies* **9** 14
- Elvidge C D, Zhizhin M, Hsu F-C and Baugh K E 2013 VIIRS Nightfire: satellite pyrometry at night *Remote Sens.* **5** 4423–49
- Fawole O G, Cai X-M and Mackenzie A R 2016 Gas flaring and resultant air pollution: a review focusing on black carbon *Environ. Pollut.* **216** 182–97
- Field R A, Soltis J and Murphy S 2014 Air quality concerns of unconventional oil and natural gas production *Environ. Sci. Process. Impacts* **16** 954–69
- Finn K, Gajda E, Perin T and Fredericks C 2017 Responsible resource development and prevention of sex trafficking: safeguarding native women and children on the Fort Berthold reservation *Harv. J. Law Gender* **40** 1–52 (<https://harvardjlg.com/wp-content/uploads/sites/19/2012/01/jlg-winter-3.pdf>)
- Franklin M, Chau K, Cushing L J and Johnston J 2019 Characterizing flaring from unconventional oil and gas operations in south Texas using satellite observations *Environ. Sci. Technol.* **53** 2220–8
- Garcia-Gonzales D A, Shonkoff S B C, Hays J and Jerrett M 2019 Hazardous air pollutants associated with upstream oil and natural gas development: a critical synthesis of current peer-reviewed literature *Annu. Rev. Public Health* **40** 283–304
- Giwa S O, Nwaokocha C N, Kuye S I and Adama K O 2019 Gas flaring attendant impacts of criteria and particulate pollutants: a case of Niger Delta region of Nigeria *J. King Saud Univ., Eng. Sci.* **31** 209–17
- Gonzalez D J X, Sherris A R, Yang W, Stevenson D K, Padula A M, Baiocchi M, Burke M, Cullen M R and Shaw G M 2020 Oil and gas production and spontaneous preterm birth in the San Joaquin Valley, CA: a case-control study *Environ. Epidemiol.* **4** e099
- Gvakharia A, Kort E A, Brandt A, Peischl J, Ryerson T B, Schwarz J P, Smith M L and Sweeney C 2017 Methane, black carbon, and ethane emissions from natural gas flares in the Bakken Shale, North Dakota *Environ. Sci. Technol.* **51** 5317–25
- Horwitz S 2014 Dark side of the boom The Washington Post (available at: www.washingtonpost.com/sf/national/2014/09/28/dark-side-of-the-boom/)
- Ite A E and Ibok U J 2013 Gas flaring and venting associated with petroleum exploration and production in the Nigeria's Niger Delta *Am. J. Environ. Protect.* **1** 70–77
- James W and Cossman J S 2017 Long-term trends in black and white mortality in the rural United States: evidence of a race-specific rural mortality penalty *J. Rural Health* **33** 21–31
- Janssen N A H et al 2011 Black carbon as an additional indicator of the adverse health effects of airborne particles compared with PM₁₀ and PM_{2.5} *Environ. Health Perspect.* **119** 1691–9
- Janssen N A H, Gerlofs-Nijland M, Lanki T, Salonen R, Cassee F, Hoek G, Fischer P, Brunekreef B and Krzyzanowski M 2012 Health effects of black carbon (World Health Organization) (available at: <https://wedocs.unep.org/handle/20.500.11822/8699>)
- Johnson M R and Coderre A R 2011 An analysis of flaring and venting activity in the Alberta upstream oil and gas industry *J. Air Waste Manage. Assoc.* **61** 190–200
- Johnston J E, Chau K, Franklin M and Cushing L 2020 Environmental justice dimensions of oil and gas flaring in South Texas: disproportionate exposure among Hispanic communities *Environ. Sci. Technol.* **54** 6289–98
- Kassotis C D, Iwanowicz L R, Akob D M, Cozzarelli I M, Mumford A C, Orem W H and Nagel S C 2016 Endocrine disrupting activities of surface water associated with a West Virginia oil and gas industry wastewater disposal site *Sci. Total Environ.* **557–558** 901–10
- Kelly-Reif K and Wing S 2016 Urban-rural exploitation: an underappreciated dimension of environmental injustice *J. Rural Stud.* **47** 350–8

- Kim K-H, Jahan S A, Kabir E and Brown R J C 2013 A review of airborne polycyclic aromatic hydrocarbons (PAHs) and their human health effects *Environ. Int.* **60** 71–80
- Kindziarski W B 1999 Importance of human environmental exposure to hazardous air pollutants from gas flares *Environ. Rev.* **8** 41–62
- Leahey D M, Preston K and Strosher M 2001 Theoretical and observational assessments of flare efficiencies *J. Air Waste Manage. Assoc.* **51** 1610–6
- Long A S, Hanlon A L and Pellegrin K L 2018 Socioeconomic variables explain rural disparities in US mortality rates: implications for rural health research and policy *SSM—Popul. Health* **6** 72–74
- Lupo P J et al (for the National Birth Defects Prevention Study) 2012 Maternal occupational exposure to polycyclic aromatic hydrocarbons: effects on gastroschisis among offspring in the national birth defects prevention study *Environ. Health Perspect.* **120** 910–5
- Lupo P J, Symanski E, Waller D K, Chan W, Langlois P H, Canfield M A and Mitchell L E 2011 Maternal exposure to ambient levels of benzene and neural tube defects among offspring: Texas, 1999–2004 *Environ. Health Perspect.* **119** 397–402
- Macey G P, Breech R, Chernaik M, Cox C, Larson D, Thomas D and Carpenter D O 2014 Air concentrations of volatile compounds near oil and gas production: a community-based exploratory study *Environ. Health* **13** 82
- Manson S, Schroeder J, Van Riper D and Ruggles S 2018 National Historical Geographic Information System: version 13.0 (available at: www.ipums.org/projects/ipums-nhgis/d050.V13.0)
- Mcewen J D N and Johnson M R 2012 Black carbon particulate matter emission factors for buoyancy-driven associated gas flares *J. Air Waste Manage. Assoc.* **62** 307–21
- Mckenzie L M, Guo R, Witter R Z, Savitz D A, Newman L S and Adgate J L 2014 Birth outcomes and maternal residential proximity to natural gas development in rural Colorado *Environ. Health Perspect.* **122** 412–7
- Mennis J 2003 Generating surface models of population using dasymetric mapping *Prof. Geogr.* **55** 31–42
- Nwoye C I, Nwakpa S O, Nwosu I E, Odo J U, Chinwuko E C and Idenyi N E 2014 Multi-factorial analysis of atmospheric noise pollution level based on emitted carbon and heat radiation during gas flaring *J. Atmos. Pollut.* **2** 22–29
- Roest G S and Schade G W 2020 Air quality measurements in the western Eagle Ford Shale *Elem. Sci. Anth.* **8** 18
- Schade G W and Roest G 2018 Source apportionment of non-methane hydrocarbons, NO_x and H₂S data from a central monitoring station in the Eagle Ford shale, Texas *Elem. Sci. Anth.* **6** 35
- Schmidt C W 2013 Estimating wastewater impacts from fracking *Environ. Health Perspect.* **121** A117
- Singh G K and Siahpush M 2014 Widening rural–urban disparities in life expectancy, U.S., 1969–2009 *Am. J. Preventive. Med.* **46** e19–29
- Stacy S L, Brink L L, Larkin J C, Sadovsky Y, Goldstein B D, Pitt B R and Talbott E O 2015 Perinatal outcomes and unconventional natural gas operations in Southwest Pennsylvania *PLoS One* **10** e0126425
- Stohl A, Klimont Z, Eckhardt S, Kupiainen K, Shevchenko V B, Kopeikin V M and Novigatsky A N 2013 Black carbon in the Arctic: the underestimated role of gas flaring and residential combustion emissions *Atmos. Chem. Phys.* **13** 8833–55
- Strosher M 1996 *Investigations of flare gas emissions in Alberta* (Calgary, Alberta: Alberta Research Council) (available at: www.ags.aer.ca/document/SPE/SPE_005.pdf)
- Tran K V, Casey J A, Cushing L J and Morello-Frosch R A 2020 Residential proximity to oil and gas development and birth outcomes in California: a retrospective cohort study of 2006–2015 births *Environ. Health Perspect.* **128** 067001–13
- Tunstall T 2015 Recent economic and community impact of unconventional oil and gas exploration and production on South Texas counties in the Eagle Ford Shale area *J. Reg. Anal. Policy* **45** 82–92
- U. S. Energy Information Administration 2020b U.S. Natural Gas Gross Withdrawals (Million Cubic Feet) (Washington, DC: US EIA) (available at: www.eia.gov/dnav/ng/hist/n9010us2m.htm)
- U.S. Energy Information Administration 2020a Crude oil production (Washington, DC: US EIA) (available at: www.eia.gov/dnav/pet/pet_crd_crdpn_adc_mdbl_m.htm)
- U.S. Energy Information Administration n.d. *Maps: Oil and Gas Exploration, Resources, and Production—Energy Information Administration* (Washington, DC: US EIA) (available at: www.eia.gov/maps/maps.htm)
- U.S. Environmental Protection Agency 2016 Integrated Science Assessment (ISA) for Oxides of Nitrogen—Health Criteria (Washington, DC: US EPA) (<https://www.epa.gov/isa/integrated-science-assessment-isa-nitrogen-dioxide-health-criteria>)
- U.S. Environmental Protection Agency 2020 Integrated Science Assessment (ISA) for Ozone and Related Photochemical Oxidants (Final Report) *EPA/600/R-20/012* (Washington, DC: US EPA) (<https://cfpub.epa.gov/ncea/isa/recordisplay.cfm?deid=348522>)
- Vesterinen H M, Morello-Frosch R, Sen S, Zeise L and Woodruff T J 2017 Cumulative effects of prenatal-exposure to exogenous chemicals and psychosocial stress on fetal growth: systematic-review of the human and animal evidence ed J Meliker *PLoS One* **12** e0176331
- Webb E, Bushkin-Bedient S, Cheng A, Kassotis C D, Balise V and Nagel S C 2014 Developmental and reproductive effects of chemicals associated with unconventional oil and natural gas operations *Rev. Environ. Health* **29** 307–18
- Weyant C L, Shepson P B, Subramanian R, Cambaliza M O L, Heimburger A, Mccabe D, Baum E, Stirn B H and Bond T C 2016 Black carbon emissions from associated natural gas flaring *Environ. Sci. Technol.* **50** 2075–81
- Whitworth K W, Kaye Marshall A and Symanski E 2018 Drilling and production activity related to unconventional gas development and severity of preterm birth *Environ. Health Perspect.* **126** 037006
- Willyard K A and Schade G W 2019 Flaring in two Texas shale areas: comparison of bottom-up with top-down volume estimates for 2012–2015 *Sci. Total Environ.* **691** 243–51
- Witter R Z, Mckenzie L, Stinson K E, Scott K, Newman L S and Adgate J 2013 The use of health impact assessment for a community undergoing natural gas development *Am. J. Public Health* **103** 1002–10
- World Bank 2020 *Global Gas Flaring Tracker Report* (available at: <http://pubdocs.worldbank.org/en/503141595343850009/WB-GGFR-Report-July2020.pdf>)

Methane, Black Carbon, and Ethane Emissions from Natural Gas Flares in the Bakken Shale, North Dakota

Alexander Gvakharia,^{*,†,‡} Eric A. Kort,[†] Adam Brandt,^{‡,§} Jeff Peischl,^{§,||} Thomas B. Ryerson,^{||} Joshua P. Schwarz,^{||} Mackenzie L. Smith,[†] and Colm Sweeney[§]

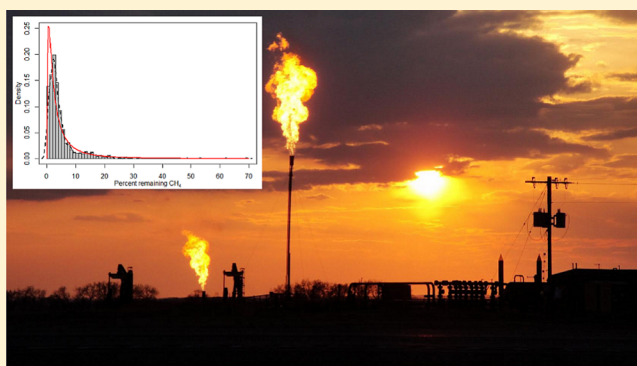
[†]Climate and Space Sciences and Engineering, University of Michigan, Ann Arbor, Michigan 48109, United States

[‡]Department of Energy Resources Engineering, Stanford University, Stanford, California 94305, United States

[§]Cooperative Institute for Research in Environmental Science, University of Colorado, Boulder, Colorado 80309, United States

^{||}NOAA ESRL Chemical Sciences Division, Boulder, Colorado 80305, United States

ABSTRACT: Incomplete combustion during flaring can lead to production of black carbon (BC) and loss of methane and other pollutants to the atmosphere, impacting climate and air quality. However, few studies have measured flare efficiency in a real-world setting. We use airborne data of plume samples from 37 unique flares in the Bakken region of North Dakota in May 2014 to calculate emission factors for BC, methane, ethane, and combustion efficiency for methane and ethane. We find no clear relationship between emission factors and aircraft-level wind speed or between methane and BC emission factors. Observed median combustion efficiencies for methane and ethane are close to expected values for typical flares according to the US EPA (98%). However, we find that the efficiency distribution is skewed, exhibiting log-normal behavior. This suggests incomplete combustion from flares contributes almost 1/5 of the total field emissions of methane and ethane measured in the Bakken shale, more than double the expected value if 98% efficiency was representative. BC emission factors also have a skewed distribution, but we find lower emission values than previous studies. The direct observation for the first time of a heavy-tail emissions distribution from flares suggests the need to consider skewed distributions when assessing flare impacts globally.



INTRODUCTION

Over 140 billion cubic meters (BCM) of gas is globally flared each year.¹ Flaring is used to dispose of gas at production and processing facilities that lack infrastructure and means to capture or use the gas. The United States flares about 8 BCM per year, with almost half of that coming from North Dakota alone.² From 2004 to 2014, the amount of gas annually flared in North Dakota increased from 0.08 to 3.7 BCM, and in 2014, about 28% of North Dakota's total produced natural gas was flared.³ Flaring has implications for the atmosphere. Although ideally, gas would be captured instead of lost, it is preferable to flare rather than vent because flaring destroys methane (CH₄) and volatile organic compounds that affect air quality, converting them to CO₂. CH₄ is a potent greenhouse gas, the second-most-important anthropogenic greenhouse gas behind CO₂ based off integrated radiative forcing.^{4,5} Flaring is not 100% efficient, and through incomplete combustion, it can be a source for CH₄ and VOCs.^{6,7} Flaring can also create black carbon (BC) as a by-product, an anthropogenic forcer of climate with public health implications.^{8–11} The World Bank recently introduced a "Zero Routine Flaring" initiative to end flaring worldwide by 2030 through government incentives and

institutional cooperation, hoping to mitigate economic losses due to flaring and relieve its burden on the atmosphere.¹²

Inventories that account for flaring often use a combustion efficiency value of 98% of the initial gas, citing an EPA technical report.^{13,14} This efficiency value assumes flare stability and can decrease based on wind speed and other factors such as flow rate or aeration. Studies have investigated flare efficiency in laboratories using scaled-down flare simulations in a controlled environment, reporting 98–99% flare combustion efficiency,^{15,16} but there have been few field studies done to assess flare efficiency and directly measure emissions in a real-world environment. Thus, scaled-up laboratory results may not be representative of real-world flaring. A study of two flare sites in Canada calculated an average observed combustion efficiency of 68 ± 7%, much lower than the assumed efficiency.¹⁷ One remote sensing study in The Netherlands found high efficiencies of 99% but only analyzed three flares, with up to

Received: October 12, 2016

Revised: April 10, 2017

Accepted: April 12, 2017

Published: April 12, 2017

30% error in the measured gas concentrations, and noted the lack of in situ data.¹⁸ There was also a comprehensive study to observe industrial flare emissions and efficiency but the tests were conducted at a flare test facility, not directly at well sites.¹⁹ To our knowledge, the only extensive study of in situ flare efficiency for CH₄ sampled ten flares in the Bakken Shale in North Dakota and one in western Pennsylvania.²⁰ This study reported high flare efficiencies up to 99.9%, but based on their identification techniques, they acknowledged a possible bias toward larger, brighter-burning, and thus more-efficient, flares.

Black carbon emissions from gas flaring have been investigated, but there are not many studies that use direct observations of flaring. Schwarz et al. (2015)¹⁰ quantified total field emissions of BC and derived an upper-bound on BC emission factor for flaring from the Bakken using the same aircraft campaign data as used in this paper. Their emission factor was obtained using BC flux calculated with a mass balance technique for the entire field. Hence, it did not target individual flares. It includes all BC sources in the region (e.g., diesel trucks, generators, limited agriculture, etc.) and is expected to provide an upper bound. Weyant et al. (2016)²¹ calculated BC emission factors from targeted flares in the same region and found an average value well below the upper bound of Schwarz et al. (2015), and, to our knowledge, this is the only previously published peer-reviewed study of BC emissions from flaring that directly sampled flares. BC emission factors have been shown to vary based on fuel chemistry and stability of the flare, necessitating the use of specific emission factors or a distribution rather than using a single average value as representative.²²

The lack of direct, in situ observations of flaring efficiency suggests that estimates of emissions from incomplete combustion may be inaccurate. Also, using a single value for flaring emission factors or combustion efficiency does not take into account the various parameters that may affect a flare,²³ and a statistically robust sample of flaring efficiency would help identify a representative distribution. Total fugitive emissions from oil and gas production and leakage can be a substantial source of atmospheric CH₄ and are underrepresented in inventories.²⁴ Studies have observed non-normal distribution of CH₄ emissions in some fields, where less than 10% of sampled sources contributed up to 50% of the sampled emissions.^{25–29} A study of flare emissions using Greenhouse Gas Reporting Program and Gas Emission Inventory data found that 100 flares out of 20 000 could be responsible for over half the emissions in the United States, but this conclusion results from the non-normal distribution of gas volume flared and not from a skewed flare combustion efficiency (which is not represented).³⁰ In addition to the non-normal distribution of gas volume flared, there may be a skewed distribution of emissions from incomplete combustion in flares based on efficiency as well.

We present an analysis of combustion efficiency and emission factors of CH₄, BC, and C₂H₆ for 37 distinct flares in the Bakken Shale Formation in North Dakota using data obtained during a May 2014 aircraft campaign, this being (to our knowledge) the largest study of flaring emissions in the field based on number of flares and the first to include C₂H₆. This gives us sufficient statistics to obtain an efficiency distribution and determine the implications for total fugitive emissions from incomplete combustion in actual field conditions.

METHODS

Flights and Instrumentation. All observations used in this analysis were made as part of the Twin Otter Projects Defining Oil–Gas Well Emissions (TOPDOWN 2014) study and were collected onboard a National Oceanic and Atmospheric Administration (NOAA) DHC-6 Twin Otter aircraft.^{10,31,32} This campaign focused on understanding the atmospheric impact of fossil fuel extraction activities. A total of 17 research flights were conducted on 11 separate days between May 12–26, 2014, totaling 40 h. Flights were typically 3–3.5 h in duration and were primarily conducted at low-altitudes (400–600 magl) within the planetary boundary layer at an average speed of 65 m/s. Vertical profiles were performed in each flight to define the mixed layer height. Flights dedicated to mass balance conducted transects around the Bakken region, and although a few flares were sampled during these transects, most of the flares were identified on “mowing-the-lawn” flights that swept across the region to target point sources as well as some flights dedicated to point source identification. Flares were circled multiple times during these flights between 400 and 600 magl, although some were sampled higher up, around 1000 magl. Flares were not specifically targeted for any particular characteristic such as size, brightness, or flaring volume. Flares were sampled over the entire region rather than in a particular cluster, giving low spatial sampling bias. However, due to the nature of the sampling, brighter flares were more easily identifiable from the plane and, thus, more likely to have been targeted. Not all passes by a flare produced a well-defined peak that could be used in the efficiency analysis. Many of the flares were sampled at a distance on the order of hundreds of meters to kilometers downwind. This gave the flare plume time to disperse and allowed us to measure large plumes over a time period of 10–20 s, providing more data per plume than if we sampled closer and lower.

CH₄, CO₂, carbon monoxide (CO), and water vapor (H₂O) were measured with a Picarro 2401-m cavity ringdown spectrometer with a sampling rate of 0.5 Hz. CH₄ was measured with an accuracy of ±1.4 ppb and a precision of ±0.2 ppb, and CO₂ was measured with an accuracy of ±0.15 ppm and a precision of ±0.03 ppm.^{33,34} An Aerodyne mini direct absorption spectrometer was used to continuously measure C₂H₆, deployed as described previously in literature^{35,36} along with hourly measurements of a standard gas to confirm stability.³² Sampling was conducted at 1 Hz with precision of <0.1 ppb and an average accuracy of ±0.5 ppb.³² Due to the Aerodyne ethane instrument having a response time of 1 s, compared to the Picarro's 2 s response time, there were sharper, narrower peaks in C₂H₆ than CO₂ and CH₄. To enable a point-by-point comparison of C₂H₆ to CO₂, a weighted moving average (WMA) was applied to the C₂H₆ data. The total integrated value of the C₂H₆ peak did not significantly change with the WMA filter, indicating conservation of mass with the method.

All trace gases are reported as dry air mole fractions, converted from the measured wet air mole fractions using water vapor observations from the Picarro. A single-particle soot photometer (SP2 by Droplet Measurement Technology Inc., Boulder, CO) was used to measure refractory black carbon (rBC) for particles containing rBC in the mass range of 0.7–160 fg. The SP2 provided 1-s rBC mass-mixing ratios with systematic uncertainty of 25%.^{10,37} A pair of differential GPS antennae on the fuselage of the Twin Otter provided aircraft

heading, altitude, latitude, longitude, ground speed, and course over ground. Wind speed was calculated as described in Conley et al. (2014),³⁸ with estimated uncertainties of ± 1 m/s in magnitude and $\pm 6^\circ$ in direction. A Rosemount deiced Total Temperature Sensor, model number 102CP2AF, measured ambient temperature. Calibration before and after the field project indicate measurement performance with precision of ± 0.2 °C and accuracy of ± 1.0 °C.

Flare Identification. We identified flares in the following ways. During the science flights, all significant events were logged, including when the plane flew by a flare. These flight notes thus provide times when a flare was visually confirmed, and these flare plumes were identified in the data for the corresponding flight and flagged. After locating all the flares confirmed by the flight notes, we searched through the remaining data to find plumes that could be possible flares but were not noted during the flight, such as smaller flares that might have been hard to see on the ground. To identify the other possible flare plumes, we looked for peaks in CO_2 where ΔCO_2 , the peak enhancement, was greater at its maximum point than 4σ of the CO_2 background variability, indicating a statistically significant elevation of CO_2 as a result of combustion from a flare. We also looked for a peak less than 20 s in time. At a mean ground speed of 65 m/s, this corresponds to a source about 3 km away using Gaussian plume theory,³⁹ which is about the distance we tended to sample where the plume still presented a robust signal above background. Figure 1 shows the research aircraft flight paths, known flare locations,³ and where we sampled plumes.

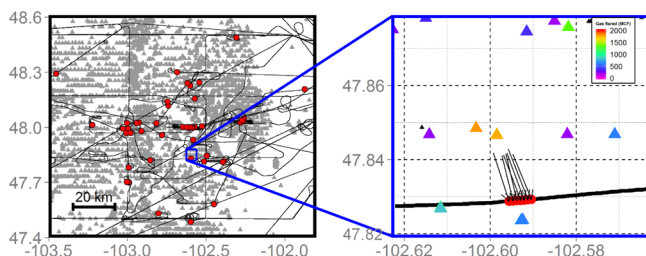


Figure 1. Left panel shows flight paths (black lines), wells with known flaring (gray triangles),³ and flare plume locations (red points) from the TOPDOWN 2014 campaign in the Bakken field in northwest North Dakota. Times when the plane circled around an area multiple times to repeatedly sample can be seen in the middle of the region. Right panel is zoomed in on a single flare plume, with flight path (black line), flare plume (red points), and wells with reported flaring (filled triangles with corresponding monthly flaring amounts). The arrows indicate the wind direction, distance from well, and flaring amount to verify that the plume was caused by flaring.

To verify if these additional plumes identified in the data were indeed caused by flaring, we co-plotted the locations of these events with all nearby wells with reported flaring and other CO_2 producers such as processing facilities and gas plants using the EPA GHG Reporting Program as seen in Figure 1. Certain flare locations were cross-checked with additional data from the VIIRS Active Fire Map and North Dakota Oil and Gas ArcIMS Viewer. Then, using Gaussian plume theory, we estimated how far away the source of a plume was based on the plume width and wind conditions, matching the plume to a possible flare source.³⁹ Although the science flights were conducted on days with steady winds, leading to low variability

in wind speed and direction, we accepted plumes that were within 20% of the theoretical distance to account for deviation in other factors such as not flying directly in the center of the diffused plume. If a plume was located downwind from a well with flaring, was not downwind of another CO_2 source, and had a width and distance consistent within 20% of Gaussian plume theory, we considered it likely due to a flare source. If a plume was not downwind of a flare at a distance consistent with Gaussian plume theory or had interference from another CO_2 source, we omitted it from the analysis. A total of 39 flare plumes were identified with the flight notes, and out of 17 additional plumes in the data, 13 were accepted using our verification method and 4 rejected for a total of 52 flare plumes from 37 unique flares.

Other sources for methane or black carbon closely collocated with flares (such as diesel engines or fugitive losses from production wells) could contribute to the observations we are attributing to flaring, and we assess their potential impact on our analysis here. Using gas composition data from over 550 samples, the average chemical plume from the Bakken was determined to be 0.7% CO_2 , 3.7% N_2 , 49% CH_4 , 21% C_2H_6 , and the rest in higher-order hydrocarbons.⁴⁰ This results in a molecular weight of about 29 g/mol, close to that of air and nearly double the weight of natural gas from other fields with higher CH_4 ratios.²¹ An unburned source of gas is therefore neutrally buoyant compared to a hot flare exhaust plume, which will rise in the atmosphere.⁴¹ However, the flare plume can entrain these other sources, mixing them as the buoyant plume rises in the atmosphere. If we assume a flare converts 98% of its hydrocarbons to CO_2 , and that enhancements near a well pad due to other emissions are 50 ppm of CH_4 and 415 ppm of CO_2 , then if the flare plume entrained a volume equal to its own (50% dilution), the resulting CH_4/CO_2 slope measured by the aircraft (see Figure 2) would change by less than 1%, smaller than the uncertainty range in fitting the slope. Considering typical values for methane and CO_2 enhancement (40 ppb and 5 ppm on average, respectively), we estimate the slope error (and, thus, the error on calculated emission factors) would be less than 1% with 10% as an upper bound. Adjusting the flare efficiency in this estimation does not significantly affect the result (using a 90% combustion efficiency, all else equal, would also have an impact of 1% on the slope). Although we cannot definitively rule out all potential contributions from such sources to the plumes we are analyzing, these considerations of possible entrainment suggest it is not significant in this analysis, though the potential impact would suggest our results may represent a lower bound for combustion efficiency.

Combustion Efficiency. Destruction efficiency and emissions factors were calculated for each flare sampled. Black carbon emission factors were determined following the methodology of Weyant et al. (2016)²¹ using eq 1:

$$EF_{\text{BC}} = 1000 \times F \frac{C_{\text{BC}}}{C_{\text{CO}_2} + C_{\text{CH}_4} + C_{\text{BC}}} \quad (1)$$

Here, C_{CO_2} , C_{CH_4} , and C_{BC} are the mass concentrations of carbon in g/m^3 for each product with the respective background removed and F is the ratio of carbon mass to total hydrocarbon mass, calculated to be 0.79 from gas composition data for the Bakken.⁴⁰ CO_2 and CH_4 data were converted from molar ratios to g/m^3 using a molar volume at standard temperature and pressure (273 K, 1013 mb) to match

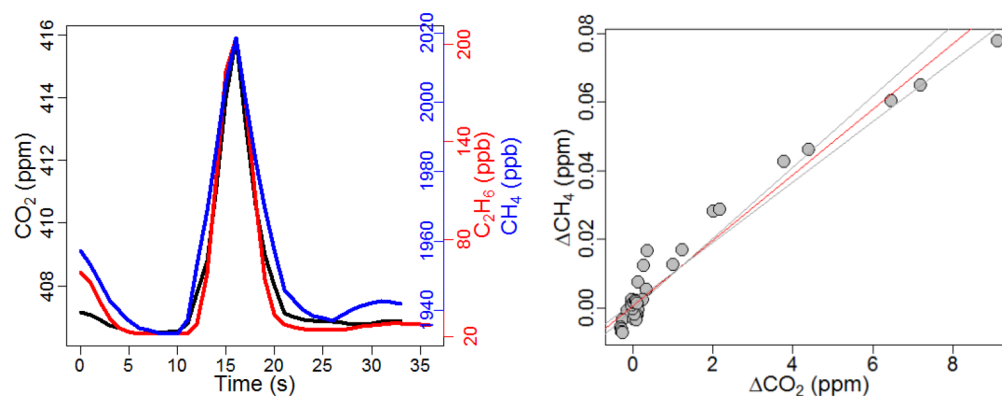


Figure 2. Example of a flaring plume with CO₂, CH₄, and C₂H₆ time series and regression to find CH₄ EF.

the conditions of the BC mass concentrations. This EF_{BC} value is given in grams of BC per kilogram of gas and can be converted to g/m³ using a gas density of 1.23 ± 0.14 kg/m³ for the composition.⁴⁰ For some of the flares we did not detect a strong BC enhancement correlated with CO₂, causing skewed or negative emission factor values. To account for this, when the peak enhancement ΔBC was below the detection limit of 4σ of the background, we used a value of half the detection limit in the EF calculation as in Weyant et al. (2016);²¹ this was observed in a third of the plumes. The measured BC concentrations were scaled up by 15% to account for accumulation-mode mass outside of the SP2 detection range, as described in Schwarz et al. (2015);¹⁰ rBC mass in either the coarse mode or a subaccumulation mode size range would not be accounted for by this adjustment. Generally, as in Schwarz et al. (2015),¹⁰ the accumulation mode size distribution is well-fit with a log-normal function, and any additional smaller or larger populations of BC particles are revealed by deviations from the log-normal fit at the smaller or larger limits of the detection range, respectively. Here, there was no evidence of additional nonaccumulation modes.

Emission factors for CH₄ and C₂H₆ were obtained by first calculating the peak enhancement of CH₄, C₂H₆, and CO₂. We calculated a mean background value for each plume using the concentration data from 5 to 10 s before the start and after the end of the plume and then subtracted the background from the plume values to obtain ΔCH_4 , ΔC_2H_6 , and ΔCO_2 . ΔCH_4 and ΔC_2H_6 were fit with a Reduced Major Axis (RMA) regression to ΔCO_2 for each peak to obtain the emission factor in ppm of CH₄ or C₂H₆ per ppm of CO₂.²⁰ Figure 2 shows an example plume from a flare and its CH₄ regression. Regressions were well-correlated with 10–20 data points in each flare plume. Uncertainty in EF for CH₄ and C₂H₆ was given by 95% confidence intervals from the regression. For all plumes, EF_{BC} from eq 1 linearly correlated with the slope of BC versus CO₂ with an R^2 of 0.97. This fit was used to derive uncertainty in EF_{BC} from 95% confidence intervals of the regression of BC and CO₂.

We calculated the destruction removal efficiency (DRE) following the methodology of Caulton et al. (2014)²⁰ using eq 2, with a small correction to report the value as the fraction of gas destroyed rather than remaining.

$$\text{DRE (\%)} = \left(1 - \frac{\mu_{CH_4}}{((X) \times \mu_{CO_2}) + \mu_{CH_4}} \right) \times 100 \quad (2)$$

μ_{CH_4} and μ_{CO_2} are the gas concentrations in ppm, and X is the carbon fraction of CH₄ in the total fuel gas before combustion. From gas composition data for the field,⁴⁰ the value of X is 0.26 ± 0.05 for CH₄.

This DRE calculation was done two ways. First, by integrating over the entire peak to obtain a DRE value from the total integrated amount of CH₄ and CO₂. Second, by calculating the DRE value for each point in the peak individually to get an aggregate DRE data set as seen in Caulton et al. (2014).²⁰ The respective baseline values were removed from each gas concentration in both methods. Because the integral method calculates DRE using the average concentration over the sampling time of the gases in the plume, and the point-by-point mean represents the average instantaneous DRE, a significant divergence between the results would be indicative of a potential problem with the approach. For all flares, the integrated DRE differed from the mean point-by-point DRE by 1% on average, demonstrating robustness between the two methods. C₂H₆ DRE was also calculated using both methods, with $X = 0.23 \pm 0.03$ for C₂H₆. The effect of X 's variability on the DRE is small and within the calculated uncertainty for DRE.

Detection Threshold. We compared the standard deviation of CH₄ background and the maximum peak CO₂ enhancement to calculate a "noise DRE" using eq 2 to assess the impact of a potential signal produced by background variability on the DRE. The distribution suggests a sensitivity threshold around 99%. We compared the sensitivity distribution to the measured DRE distribution, and an analysis of variance between the two produced a p value of 9×10^{-7} , suggesting that they are statistically significantly different. Thus, it would be difficult to distinguish measured DRE values of greater than 99% as significant compared to background variability, but values less than 99%, as we have observed, are robustly detectable with our approach. There is a trade-off between our sampling approach and the one used by Caulton et al. (2014),²⁰ where they flew lower and closer to the flares. With our flights, we obtained more points in each plume, allowing us to calculate regression lines for emission factors. However, we encountered a lower signal-to-noise ratio, making it more difficult to precisely measure the DRE of very efficient flares. We used the difference between 100% and the DRE calculated using the sensitivity as a proxy for DRE uncertainty in each individual flare.

RESULTS

Emission Factors. Figure 3 shows the calculated CH_4 and C_2H_6 emission factors plotted against mean aircraft-level wind

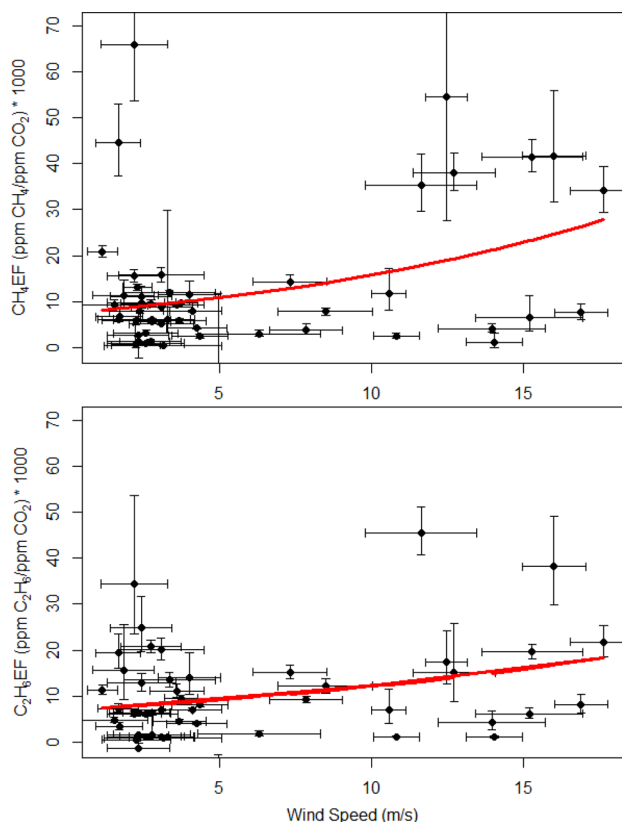


Figure 3. CH_4 and C_2H_6 EF plotted against wind speed for all plumes, with an exponential fit in red. Error bars represent 95% confidence intervals in EF and 1σ in wind speed.

speed for all flare plumes. Previous laboratory flare studies have observed a strong nonlinear dependence of inefficiency on crosswind speed,^{15,16} and Caulton et al. (2014)²⁰ observed a weak relationship in the flares they sampled in the field. Considering our observed emission factors and crosswind speeds, we find similar results to Caulton et al. (2014). An exponential fit of our data suggests a weak dependence, with parts of the data possibly following different distinct curves. A Pearson correlation analysis of the data and the exponential fit

produced a weak correlation coefficient (0.34). Gas exit velocity and flare parameters like the stack diameter can affect the inefficiency curve and may be the reason for the apparent presence of multiple curves, but unfortunately, these values were not known for our sampled flares. More-specific knowledge of the gas composition and flow rate would potentially be illuminating for the possible bimodal distribution in CH_4 EF of low-efficiency emitters (>30 ppb/ppm) and high-efficiency emitters (0–20 ppb/ppm), but we can only hypothesize without detailed information on specific flares at time of our sampling.

Some flares were circled repeatedly or revisited on different days, and so we transected multiple plumes from the same flare. The calculated EF for the flare was not consistent between different plumes, suggesting fluctuation in the efficiency. Caulton et al. (2014) found large overall variability in CH_4 EF and inconsistency between sampling on different days but attribute the variability to the small sample size of their plumes.²⁰ Weyant et al. (2016) reported inconsistent emissions of BC for flares sampled on different days, and observed large variability in BC EF for multiple passes of the same flare, citing variability in gas flow rate and gas composition as possible sources.²¹ From our data alone, we cannot resolve the cause of same-flare variability, but it is apparently a feature consistent across studies.

We did not observe a clear relationship between EF and wind speed for plumes from the same flare, possibly due to factors such as flow rate or exit velocity. For some flares that were sampled multiple times, we did not get a sharp, identifiable peak in CO_2 or CH_4 on every pass, and so we were not able to analyze all possible passes. The EF calculation included background points in the regression, removing these points from the fit and forcing the line through zero did not significantly affect the results. Comparing CH_4 and C_2H_6 emission factors for each plume, we found a linear relationship with a R^2 value of 0.57, as plumes with higher emissions of CH_4 had corresponding higher emissions of C_2H_6 , suggesting that combustion efficiency is somewhat uniform across hydrocarbons.

Like Weyant et al. (2016),²¹ we did not observe a dependence between BC emission factor and CH_4 EF for each plume. Elevated CH_4 emissions from a flare do not necessarily indicate higher or lower BC emission. Adding in an ethane term to eq 1 did not significantly change the BC EF

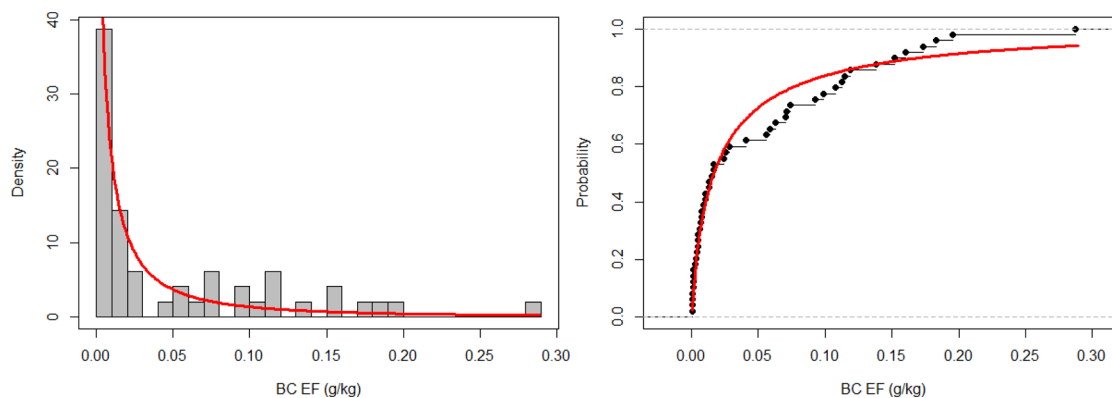


Figure 4. On the left, a histogram of black carbon emission factor for all flare plumes, with log-normal density (red line). On the right, distribution function of BC EF in black with log-normal distribution function in red.

calculation, as the ppm-order enhancement of CO₂ dominates the ppb-order enhancement of C₂H₆ and CH₄.

Figure 4 shows the distribution and probability function of BC emission factor in g BC/kg gas. The distribution is right-skewed, matching the results of Weyant et al. (2016),²¹ and was fit with a log-normal density using a maximum-likelihood method. The log-normal distribution function is given by

$$f(x) = \frac{1}{\sqrt{(2\pi)\sigma x}} e^{-((\log x - \mu)^2 / (2\sigma^2))} \quad (3)$$

μ and σ are the mean and standard deviation of the logarithm. A Pearson correlation analysis between the BC emission factor probability distribution and the log-normal distribution resulted in a correlation coefficient of 0.96. We present the log-normal fit as a way to illustrate the skewed distribution and provide a quantitative representation. Results derived from the combustion efficiency distribution use the raw distribution rather than an approximation with the log-normal fit.

We report BC EF from flares in g/kg, which is grams of BC produced per kilogram of hydrocarbons in the fuel gas. The values ranged from 0.0004 to 0.287 g/kg. We can convert from g/kg to g/m³ using a flared gas density of 1.23 ± 0.14 kg/m³,⁴⁰ allowing us to express BC EF in terms of gas flared volume and to compare the results with previous studies. Even with the observation of a right-skewed distribution, our analysis finds lower BC emissions than previously reported. Schwarz et al. (2015)¹⁰ provided an estimate for all the BC sources in the Bakken of 0.57 ± 0.14 g/m³. This upper bound on flaring is twice the highest emission value we observed (Figure 4). Similarly, laboratory analysis by McEwen et al. (2012)²² reported emissions much larger than we observe (0.51 g/m³, off scale in Figure 4). The mean value of 0.13 ± 0.36 g/m³ measured with an SP2 by Weyant et al. (2016)²¹ is within our observed range, though it falls within the top 20% of emitters we observed. Our observed in-field flares thus appear to have produced less BC than would be predicted from previous studies. The median, mean, and standard deviation of the mean BC emission factor we observed were 0.021 g/m³ and 0.066 ± 0.009 g/m³ (or 0.017 g/kg and 0.053 ± 0.008 g/kg), respectively, though given the skewed distribution care needs to be taken in interpreting these values. Given that 3.7 BCM of gas was flared in the Bakken field in 2014,³ applying that to the entire distribution of BC EF in g/m³ suggests total BC emissions from flaring of 0.24 Gg BC/year. However, the top quartile of flares contribute disproportionately, 0.17 Gg BC/year, which is 70% of the total emissions from flares. Overall, our emission rate of 0.24 Gg BC/year is two-thirds the rate of 0.36 Gg BC/year calculated by Weyant et al. (2016)²¹ for flares and 17% of the total Bakken emission rate (1.4 Gg BC/year) reported by Schwarz et al. (2015).¹⁰ Based on these results, using a single emission factor to estimate emissions from flares in a region does not properly represent the wide variability in emissions that may be present. Total emissions from flaring could potentially be substantially reduced if the least efficient flares alone are identified and addressed.

Combustion Efficiency. For methane and ethane, the percent of gas remaining provides a useful metric for flare efficiency; this is simply 100-DRE. In Figure 5 the distribution of percent remaining CH₄ and C₂H₆ is illustrated, and a log-normal relationship is apparent. As with emission factors, we found a linear relationship between CH₄ and C₂H₆ DRE for each plume, with a R² of 0.53.

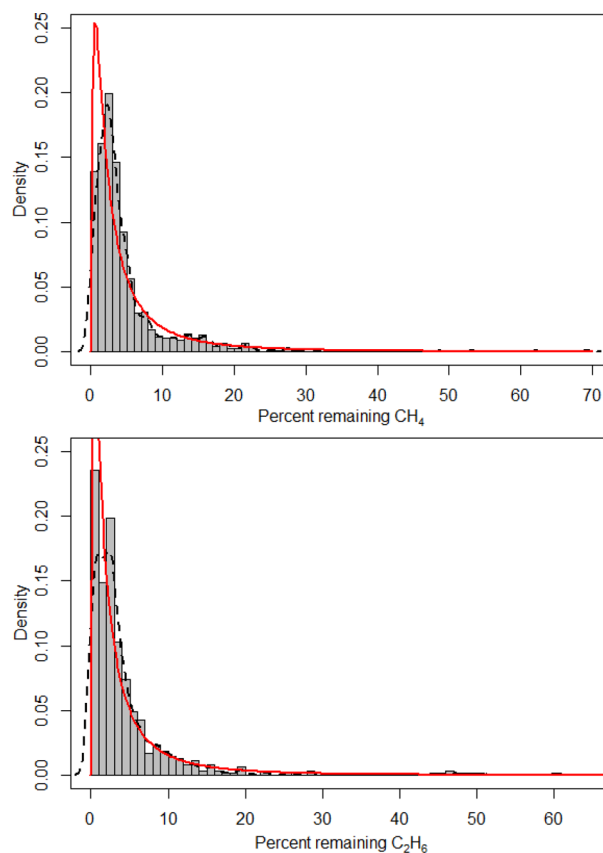


Figure 5. Histogram of remaining CH₄ and C₂H₆ (100-DRE) with density curve (dashed black) and log-normal fit (red). These distributions were integrated to calculate the emissions due to incomplete combustion.

A Pearson correlation analysis of the DRE probability distributions and the log-normal fit distribution produced a correlation coefficient of 0.99 for both CH₄ and C₂H₆. The distribution of CH₄ and C₂H₆ emission factors, which are theoretically consistent with the DRE calculations, also exhibit a skewed distribution though a log-normal relationship is not as apparent. The median DRE for CH₄ is 97.14 ± 0.37 using the integral method and 96.99 ± 0.23 using the aggregate data set. For C₂H₆ the median DRE is 97.33 ± 0.27 and 97.36 ± 0.25 , respectively. These median values are close to the expected efficiency (98%), but the right-skewed distribution indicates that 98% is not a representative destruction efficiency and would overpredict methane and ethane destruction.

We can assess the impact of this observed skewed distribution by considering the contribution of incomplete flare combustion to total field methane and ethane emissions. Using aircraft data and a mass balance technique, Peischl et al. (2016)³¹ calculated a methane flux for the Bakken region that extrapolates to an annual flux of 0.25 ± 0.05 Tg CH₄/year. As with black carbon, we can use reported flaring gas volumes for North Dakota in 2014³ and integrate the distribution of observed DRE values to produce an estimated emission of methane from incomplete combustion of 0.052 Tg CH₄/year, or $21\% \pm 4\%$ of the total emissions reported by Peischl et al. (2016), using the uncertainty bound on the flux calculation. This is more than double the contribution one would find if the expected value of 98% was assumed representative of the field, which would predict emissions representing $8\% \pm 1.6\%$ of the total field emissions. Caulton et al. (2014) reported much-

higher combustion efficiencies, and applying their median 99.98% value would suggest only a fraction of a percent (0.13% \pm 0.03%) of the total field emissions was from incomplete combustion in flares.

We performed the same analysis for ethane, and compared with the total field emissions estimate of 0.23 ± 0.07 Tg C₂H₆/year reported in Kort et al. (2016).³² Again our observed combustion efficiencies suggest incomplete combustion from flares contributes substantially to total field emissions, 17% \pm 5% of the total emissions (0.039 Tg/year), more than double that predicted by using 98% as a representative value.

The observed log-normal distribution results in a disproportionate impact from flares exhibiting poor combustion efficiencies. We find the top quartile of methane emitters contribute 0.036 Tg CH₄/year, which is 69% of total emissions from incomplete flare combustion (and 14% of the total field emissions). Similarly, for ethane, the top quartile of emitters contributes 0.026 Tg C₂H₆/year, which is 66% of the total emissions from incomplete flare combustion (and 12% of total field emissions).

Why do we find higher methane emissions and lower black carbon emissions than other studies conducted in the Bakken shale?^{10,20,21} We cannot definitively pinpoint the reason. We sampled in the same subregion of the Bakken as Caulton et al. (2014),²⁰ though we did not sample any of the same flares they did, and our campaign was 2 years after theirs. Weyant et al. (2016)²¹ did not report specific flare locations but were likely in the same subregion as well 2 months before our campaign.

There is a difference in sampling methods that could contribute. Caulton et al. (2014) flew low and close to the flares, although specific altitudes and distances are not reported.²⁰ As we did not specifically target larger (and so potentially more-efficient) flares, our approach makes it more likely to sample higher-emitting flares. Weyant et al. (2016) also likely flew closer to the flares than we did, although at a slower speed (45 m/s) than at which we typically sampled (65 m/s).²¹ We did not observe a clear correlation between sampling distance and combustion efficiency in our data, but it certainly affects variables such as plume entrainment, other emissions sources, turbulence, and environmental factors.

The largest source of discrepancy in results is likely that relatively few flares have been sampled: 26 (85 passes) by Weyant et al. (2016),²¹ 10 by Caulton et al. (2014),²⁰ and 37 (52 passes) in our study, and thus, there is large representation error. In our study, we attempt a statistical sampling for greater representativeness, but given that there were over 5500 wells with reported flaring in the Bakken in 2014,³ 37 independent flares only represents 0.6% of active flares. Thus, we think our results should be considered in concert with the Weyant and Caulton analyses, and our data should be considered in aggregate. In doing so, it would subtly change our total estimated contribution (lower for methane and higher for black carbon), but the observed log-normal distribution result would not change.

GLOBAL IMPLICATIONS

Our sampling provides sufficient statistics to observe a heavy-tail distribution of combustion efficiencies. This heavy-tail characteristic has been observed and reported for methane emissions from the oil and gas sector,^{25–27,29,42} but this represents a first observation of the heavy-tail for flaring emissions of methane and ethane. This has important implications for current and future contributions from flaring

activities. To illustrate, let us consider if our observed distribution were globally representative. Globally, 143 ± 13.6 BCM of gas is flared annually.⁴³ If 98% destruction removal efficiency were representative of every flare, that would correspond to a range in methane emissions of 1.14–1.90 Tg CH₄/year for a gas composition range of 60%–100% CH₄. Applying our observed distribution, that range changes to 2.78–4.64 Tg CH₄/year, more than doubling the amount emitted. In assessing the climate and air quality impacts of flaring, it is critical that skewed distributions are accounted for in the cases of methane, ethane, and black carbon. Although our specific observed emissions factors and efficiencies are likely only representative of the Bakken field, the observations of a skewed distribution is likely general.

AUTHOR INFORMATION

Corresponding Author

*Phone: (734) 764-7099; e-mail: agvak@umich.edu.

ORCID

Alexander Gvakharia: 0000-0003-1260-4744

Adam Brandt: 0000-0002-2528-1473

Notes

The authors declare no competing financial interest.

ACKNOWLEDGMENTS

Data from the aircraft campaign reported in the manuscript are archived and available at <http://www.esrl.noaa.gov/csd/groups/csd7/measurements/2014topdown/>. This project was supported by the NOAA AC4 program under grant no. NA14OAR0110139 and NASA grant no. NNX14AI87G. J.P. and T.R. were supported in part by the NOAA Climate Program Office and in part by the NOAA Atmospheric Chemistry, Carbon Cycle, and Climate Program. We thank NOAA Aircraft Operations Center staff and flight crew for their efforts in helping collect these data.

REFERENCES

- (1) Elvidge, C. D.; Ziskin, D.; Baugh, K. E.; Tuttle, B. T.; Ghosh, T.; Pack, D. W.; Erwin, E. H.; Zhizhin, M. A Fifteen Year Record of Global Natural Gas Flaring Derived from Satellite Data. *Energies* **2009**, *2*, 595.
- (2) U.S. Energy Information Administration. Natural Gas Gross Withdrawals and Production. https://www.eia.gov/dnav/ng/ng_prod_sum_a_EPG0_VGV_mmcf_a.htm (accessed on 4/13/2016).
- (3) North Dakota State Government. North Dakota Drilling and Production Statistics. <https://www.dmr.nd.gov/oilgas/stats/statisticsvw.asp> (accessed on 4/13/2016).
- (4) IPCC. In *Climate Change 2013: The Physical Science Basis. Contribution of Working Group I to the Fifth Assessment Report of the Intergovernmental Panel on Climate Change*; Stocker, T., Qin, D., Plattner, G.-K., Tignor, M., Allen, S., Boschung, J., Nauels, A., Xia, Y., Bex, V., Midgley, P., Eds.; Cambridge University Press: Cambridge, United Kingdom, 2013; Chapter SPM, p 1–30.
- (5) Shindell, D. T.; Faluvegi, G.; Koch, D. M.; Schmidt, G. A.; Unger, N.; Bauer, S. E. Improved Attribution of Climate Forcing to Emissions. *Science* **2009**, *326*, 716–718.
- (6) Ismail, O.; Umukoro, G. Global Impact of Gas Flaring. *Energy Power Eng.* **2012**, *4*, 290–302.
- (7) Simpson, I. J.; Andersen, M. P. S.; Meinardi, S.; Bruhwiler, L.; Blake, N. J.; Helmig, D.; Rowland, F. S.; Blake, D. R. Long-term decline of global atmospheric ethane concentrations and implications for methane. *Nature* **2012**, *488*, 490–494.
- (8) Bond, T. C.; Doherty, S. J.; Fahey, D. W.; Forster, P. M.; Berntsen, T.; DeAngelo, B. J.; Flanner, M. G.; Ghan, S.; Kärcher, B.;

- Koch, D.; Kinne, S.; Kondo, Y.; Quinn, P. K.; Sarofim, M. C.; Schultz, M. G.; Schulz, M.; Venkataraman, C.; Zhang, H.; Zhang, S.; Bellouin, N.; Guttikunda, S. K.; Hopke, P. K.; Jacobson, M. Z.; Kaiser, J. W.; Klimont, Z.; Lohmann, U.; Schwarz, J. P.; Shindell, D.; Storelvmo, T.; Warren, S. G.; Zender, C. S. Bounding the role of black carbon in the climate system: A scientific assessment. *J. Geophys. Res., [Atmos.]* **2013**, *118*, 5380–5552.
- (9) Stohl, A.; Klimont, Z.; Eckhardt, S.; Kupiainen, K.; Shevchenko, V. P.; Kopeikin, V. M.; Novigatsky, A. N. Black carbon in the Arctic: the underestimated role of gas flaring and residential combustion emissions. *Atmos. Chem. Phys.* **2013**, *13*, 8833.
- (10) Schwarz, J. P.; Holloway, J. S.; Katich, J. M.; McKeen, S.; Kort, E. A.; Smith, M. L.; Ryerson, T. B.; Sweeney, C.; Peischl, J. Black Carbon Emissions from the Bakken Oil and Gas Development Region. *Environ. Sci. Technol. Lett.* **2015**, *2*, 281–285.
- (11) Anenberg, S. C.; Schwartz, J.; Shindell, D.; Amann, M.; Faluvegi, G.; Klimont, Z.; Janssens-Maenhout, G.; Pozzoli, L.; van Dingenen, R.; Vignati, E.; Emberson, L.; Muller, N. Z.; West, J. J.; Williams, M.; Demkine, V.; Hicks, W. K.; Kuylenstierna, J.; Raes, F.; Ramanathan, V. Global air quality and health co-benefits of mitigating near-term climate change through methane and black carbon emission controls. *Environ. Health Perspect.* **2012**, *120*, 831–839.
- (12) The World Bank. Zero Routine Flaring by 2030. <http://www.worldbank.org/en/programs/zero-routine-flaring-by-2030> (accessed on 4/13/2016).
- (13) U.S. EPA Office of Air Quality Planning and Standards (OAQPS). Parameters for Properly Designed and Operated Flares. <https://www3.epa.gov/airtoxics/flare/2012flaretechreport.pdf> (accessed on 4/13/2016).
- (14) Emission Standards Division. U.S. Environmental Protection Agency, Office of Air Radiation, OAQPS, Basis and Purpose Document on Specifications For Hydrogen-Fueled Flares. http://www.tceq.state.tx.us/assets/public/implementation/air/rules/Flare/Resource_5.pdf (accessed on 4/13/2016).
- (15) Johnson, M.; Kostiuk, L. Efficiencies of low-momentum jet diffusion flames in crosswinds. *Combust. Flame* **2000**, *123*, 189–200.
- (16) Johnson, M.; Kostiuk, L. A parametric model for the efficiency of a flare in crosswind. *Proc. Combust. Inst.* **2002**, *29*, 1943–1950.
- (17) Leahey, D. M.; Preston, K.; Stroscher, M. Theoretical and observational assessments of flare efficiencies. (Technical Paper). *J. Air Waste Manage. Assoc.* **2001**, *51*, 1610.
- (18) Haus, R.; Wilkinson, R.; Heland, J.; Schafer, K. Remote sensing of gas emissions on natural gas flares. *Pure Appl. Opt.* **1998**, *7*, 853.
- (19) Knighton, W. B.; Herndon, S. C.; Franklin, J. F.; Wood, E. C.; Wormhoudt, J.; Brooks, W.; Fortner, E. C.; Allen, D. T. Direct measurement of volatile organic compound emissions from industrial flares using real-time online techniques: Proton Transfer Reaction Mass Spectrometry and Tunable Infrared Laser Differential Absorption Spectroscopy. *Ind. Eng. Chem. Res.* **2012**, *51*, 12674–12684.
- (20) Caulton, D. R.; Shepson, P. B.; Cambaliza, M. O.; McCabe, D.; Baum, E.; Stirm, B. H. Methane Destruction Efficiency of Natural Gas Flares Associated with Shale Formation Wells. *Environ. Sci. Technol.* **2014**, *48*, 9548–9554.
- (21) Weyant, C. L.; Shepson, P. B.; Subramanian, R.; Cambaliza, M. O. L.; Heimbürger, A.; McCabe, D.; Baum, E.; Stirm, B. H.; Bond, T. C. Black Carbon Emissions from Associated Natural Gas Flaring. *Environ. Sci. Technol.* **2016**, *50*, 2075–2081.
- (22) McEwen, J. D. N.; Johnson, M. R. Black carbon particulate matter emission factors for buoyancy-driven associated gas flares. *J. Air Waste Manage. Assoc.* **2012**, *62*, 307–321.
- (23) Kahforoushan, D.; Fatehifar, E.; Soltan, J. The Estimation of CO₂ Emission Factors for Combustion Sources in Oil and Gas Processing Plants. *Energy Sources, Part A* **2010**, *33*, 202–210.
- (24) Brandt, A. R.; Heath, G. A.; Kort, E. A.; O'Sullivan, F.; Pétron, G.; Jordaan, S. M.; Tans, P.; Wilcox, J.; Gopstein, A. M.; Arent, D.; Wofsy, S.; Brown, N. J.; Bradley, R.; Stucky, G. D.; Eardley, D.; Harriss, R. Methane Leaks from North American Natural Gas Systems. *Science* **2014**, *343*, 733–735.
- (25) Yuan, B.; Kaser, L.; Karl, T.; Graus, M.; Peischl, J.; Campos, T. L.; Shertz, S.; Apel, E. C.; Hornbrook, R. S.; Hills, A.; Gilman, J. B.; Lerner, B. M.; Warneke, C.; Flocke, F. M.; Ryerson, T. B.; Guenther, A. B.; de Gouw, J. A. Airborne flux measurements of methane and volatile organic compounds over the Haynesville and Marcellus shale gas production regions. *J. Geophys. Res., [Atmos.]* **2015**, *120*, 6271–6289.
- (26) Mitchell, A. L.; Tkacik, D. S.; Roscioli, J. R.; Herndon, S. C.; Yacovitch, T. I.; Martinez, D. M.; Vaughn, T. L.; Williams, L. L.; Sullivan, M. R.; Floerchinger, C.; Omara, M.; Subramanian, R.; Zimmerle, D.; Marchese, A. J.; Robinson, A. L. Measurements of Methane Emissions from Natural Gas Gathering Facilities and Processing Plants: Measurement Results. *Environ. Sci. Technol.* **2015**, *49*, 3219–3227.
- (27) Allen, D. T. Methane emissions from natural gas production and use: reconciling bottom-up and top-down measurements. *Curr. Opin. Chem. Eng.* **2014**, *5*, 78–83.
- (28) Brandt, A. R.; Heath, G. A.; Cooley, D. Methane Leaks from Natural Gas Systems Follow Extreme Distributions. *Environ. Sci. Technol.* **2016**, *50*, 12512–12520.
- (29) Frankenberg, C.; Thorpe, A. K.; Thompson, D. R.; Hulley, G.; Kort, E. A.; Vance, N.; Borchardt, J.; Krings, T.; Gerilowski, K.; Sweeney, C.; Conley, S.; Bue, B. D.; Aubrey, A. D.; Hook, S.; Green, R. O. Airborne methane remote measurements reveal heavy-tail flux distribution in Four Corners region. *Proc. Natl. Acad. Sci. U. S. A.* **2016**, *113*, 9734–9739.
- (30) Allen, D. T.; Smith, D.; Torres, V. M.; Saldaña, F. C. Carbon dioxide, methane and black carbon emissions from upstream oil and gas flaring in the United States. *Curr. Opin. Chem. Eng.* **2016**, *13*, 119–123. SI:13 Energy and Environmental Engineering/Reaction engineering and catalysis 2016.
- (31) Peischl, J.; Karion, A.; Sweeney, C.; Kort, E. A.; Smith, M. L.; Brandt, A. R.; Yeskoo, T.; Aikin, K. C.; Conley, S. A.; Gvakharia, A.; Trainer, M.; Wolter, S.; Ryerson, T. B. Quantifying atmospheric methane emissions from oil and natural gas production in the Bakken shale region of North Dakota. *J. Geophys. Res., [Atmos.]* **2016**, *121*, 6101–6111.
- (32) Kort, E. A.; Smith, M. L.; Murray, L. T.; Gvakharia, A.; Brandt, A. R.; Peischl, J.; Ryerson, T. B.; Sweeney, C.; Travis, K. Fugitive emissions from the Bakken shale illustrate role of shale production in global ethane shift. *Geophys. Res. Lett.* **2016**, *43*, 4617–4623.
- (33) Karion, A.; Sweeney, C.; Kort, E. A.; Shepson, P. B.; Brewer, A.; Cambaliza, M.; Conley, S. A.; Davis, K.; Deng, A.; Hardesty, M.; Herndon, S. C.; Lauvaux, T.; Lavoie, T.; Lyon, D.; Newberger, T.; Pétron, G.; Rella, C.; Smith, M.; Wolter, S.; Yacovitch, T. I.; Tans, P. Aircraft-Based Estimate of Total Methane Emissions from the Barnett Shale Region. *Environ. Sci. Technol.* **2015**, *49*, 8124–8131.
- (34) Karion, A.; Sweeney, C.; Wolter, S.; Newberger, T.; Chen, H.; Andrews, A.; Kofler, J.; Neff, D.; Tans, P. Long-term greenhouse gas measurements from aircraft. *Atmos. Meas. Tech.* **2013**, *6*, 511.
- (35) Yacovitch, T. I.; Herndon, S. C.; Roscioli, J. R.; Floerchinger, C.; McGovern, R. M.; Agnese, M.; Pétron, G.; Kofler, J.; Sweeney, C.; Karion, A.; Conley, S. A.; Kort, E. A.; Nähle, L.; Fischer, M.; Hildebrandt, L.; Koeth, J.; McManus, J. B.; Nelson, D. D.; Zahniser, M. S.; Kolb, C. E. Demonstration of an Ethane Spectrometer for Methane Source Identification. *Environ. Sci. Technol.* **2014**, *48*, 8028–8034.
- (36) Smith, M. L.; Kort, E. A.; Karion, A.; Sweeney, C.; Herndon, S. C.; Yacovitch, T. I. Airborne ethane observations in the Barnett Shale: Quantification of ethane flux and attribution of methane emissions. *Environ. Sci. Technol.* **2015**, *49*, 8158–8166.
- (37) Schwarz, J. P.; Spackman, J. R.; Gao, R. S.; Perring, A. E.; Cross, E.; Onasch, T. B.; Ahern, A.; Wrobel, W.; Davidovits, P.; Olfert, J.; Dubey, M. K.; Mazzoleni, C.; Fahey, D. W. The Detection Efficiency of the Single Particle Soot Photometer. *Aerosol Sci. Technol.* **2010**, *44*, 612–628.
- (38) Conley, S. A.; Faloona, I. C.; Lenschow, D. H.; Karion, A.; Sweeney, C. A Low-Cost System for Measuring Horizontal Winds

from Single-Engine Aircraft. *J. Atmos. Oceanic Technol.* **2014**, *31*, 1312–1320.

(39) Zannetti, P. *Air Pollution Modeling*, 1st ed.; Springer US: New York City, New York, 1990.

(40) Brandt, A. R.; Yeskoo, T.; McNally, M. S.; Vafi, K.; Yeh, S.; Cai, H.; Wang, M. Q. Energy Intensity and Greenhouse Gas Emissions from Tight Oil Production in the Bakken Formation. *Energy Fuels* **2016**, *30*, 9613–9621.

(41) Beychok, M. R. *Fundamentals Of Stack Gas Dispersion*, 4th ed.; Milton R. Beychok: Irvine, CA, 2005; pp 1–193.

(42) Subramanian, R.; Williams, L. L.; Vaughn, T. L.; Zimmerle, D.; Roscioli, J. R.; Herndon, S. C.; Yacovitch, T. I.; Floerchinger, C.; Tkacik, D. S.; Mitchell, A. L.; Sullivan, M. R.; Dallmann, T. R.; Robinson, A. L. Methane Emissions from Natural Gas Compressor Stations in the Transmission and Storage Sector: Measurements and Comparisons with the EPA Greenhouse Gas Reporting Program Protocol. *Environ. Sci. Technol.* **2015**, *49*, 3252–3261.

(43) Elvidge, C. D.; Zhizhin, M.; Baugh, K.; Hsu, F.-C.; Ghosh, T. Methods for Global Survey of Natural Gas Flaring from Visible Infrared Imaging Radiometer Suite Data. *Energies* **2016**, *9*, 14.

TRIBAL COMMUNITIES AT RISK



THE
DISPROPORTIONATE
IMPACTS OF OIL AND
GAS AIR POLLUTION
ON TRIBAL AIR
QUALITY

CLEANAIR
TASK FORCE

TRIBAL AIR QUALITY

A new analysis of public data shows that Native American communities often face disproportionate health impacts from air pollution from the oil and gas industry. Meanwhile Interior Secretary Ryan Zinke and EPA Administrator Scott Pruitt are seeking to eliminate federal rules designed to limit waste and air pollution from this industry on tribal lands.

In the United States, the oil and gas industry dumps millions of tons of air pollutants into our air each year. On tribal lands alone, this mix of pollutants includes **18.4 billion cubic feet of methane**, a potent climate pollutant and the primary component of natural gas. In fact, the total amount of natural gas emitted and flared on tribal lands would fetch \$100 million if it were brought to market and generate millions in royalty revenues for tribes each year.



**MEMBERS OF THE NAVAJO NATION.
SOURCE: ENVIRONMENTAL DEFENSE FUND**

**LIKELIHOOD OF LIVING WITHIN
A ½ MILE OF AN OIL AND GAS
FACILITY COMPARED TO
ENCOMPASSING STATE(S)**

**2X
MORE
LIKELY**

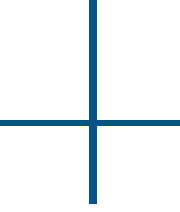
**FORT BERTHOLD INDIAN
RESERVATION**

**2X
MORE
LIKELY**

**NAVAJO NATION (UTAH &
NEW MEXICO ONLY)**

**42X
MORE
LIKELY**

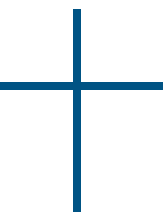
**UINTAH-OURAY
(NORTHERN UTE)**

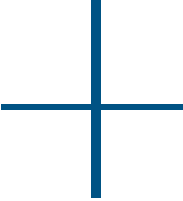


Moreover, oil and gas operations emit volatile organic compounds (VOCs) and nitrogen oxides (NOx), which combine to form ozone smog. Ozone smog poses a serious threat to children who suffer from asthma as well as seniors that have emphysema. While ozone smog is often associated with urban areas, some rural areas with oil and gas production – such as the Uinta Basin in Utah, home to the Northern Ute – have high ozone smog levels. Air pollution from the oil and gas industry also includes toxic air pollutants, such as benzene, formaldehyde, and acetaldehyde. Toxic air pollution emissions can directly affect the health of individuals living, working, or going to school adjacent to pollution sources. The impact of oil and gas air pollution is not felt equally by all communities – proximity to oil and gas operations and underlying socioeconomic factors can exacerbate the impact of this air pollution.

"If you can see pollution, you are breathing it. On Fort Berthold the oil and gas industry pollutes our air by releasing toxic gas from flares and methane leaks. Since the oil activity started in 2008, my husband and I have experienced respiratory issues and we have heard more complaints about people having coughs and worsening asthma. We are being poisoned on our own lands"

-Lisa DeVille, Mandaree, ND (Fort Berthold)





Air pollution from oil and gas facilities can have a significant impact on public health. This analysis finds that communities near active oil and gas operations experience a higher frequency of acute health impacts. We use a ½ mile radius here based on [research](#) by the Colorado School of Public Health at University of Colorado, which has found a clear correlation between health impacts and the presence of oil and gas facilities.

This is likely a conservative estimate given that other research has linked oil and gas operations to air pollution at [distances much greater than ½ mile](#).

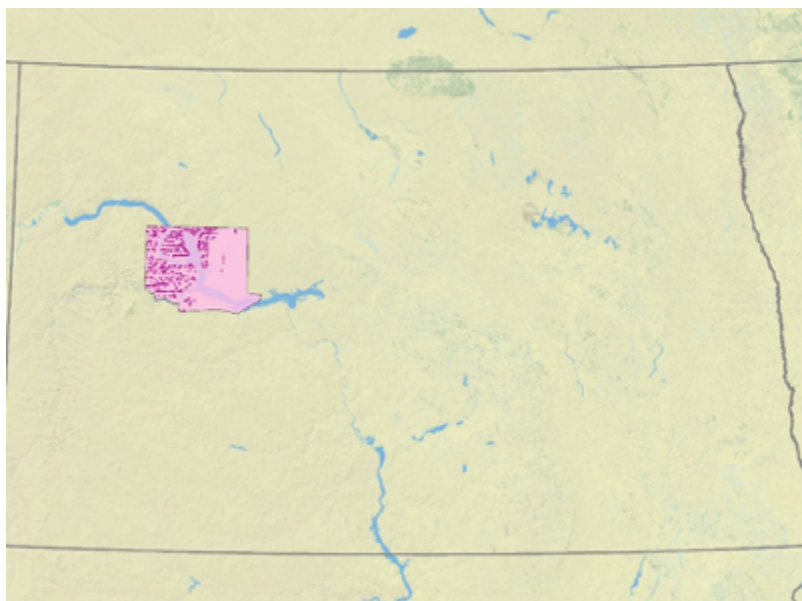
For instance, the ½ mile threat radius underestimates populations subjected to unhealthy ozone or smog pollution in areas like the Northern Ute lands in Utah's Uinta Basin. This basin was recently listed as "nonattainment" with health-based standards for ground level ozone pollution by the U.S. EPA, [a problem that has been directly linked to pollution from local oil and gas development](#). On days with unhealthy smog levels, residents across the basin are subjected to polluted air, stretching far beyond the ½ mile radius used here.

We analyzed population data and oil and gas facility information for three tribal groups on whose lands there is significant oil and gas production. We calculated how many Native Americans living on tribal lands live within a ½ mile of oil and gas facilities and compared this percent to the total population in encompassing the state(s) living within a ½ mile of oil and gas facilities.

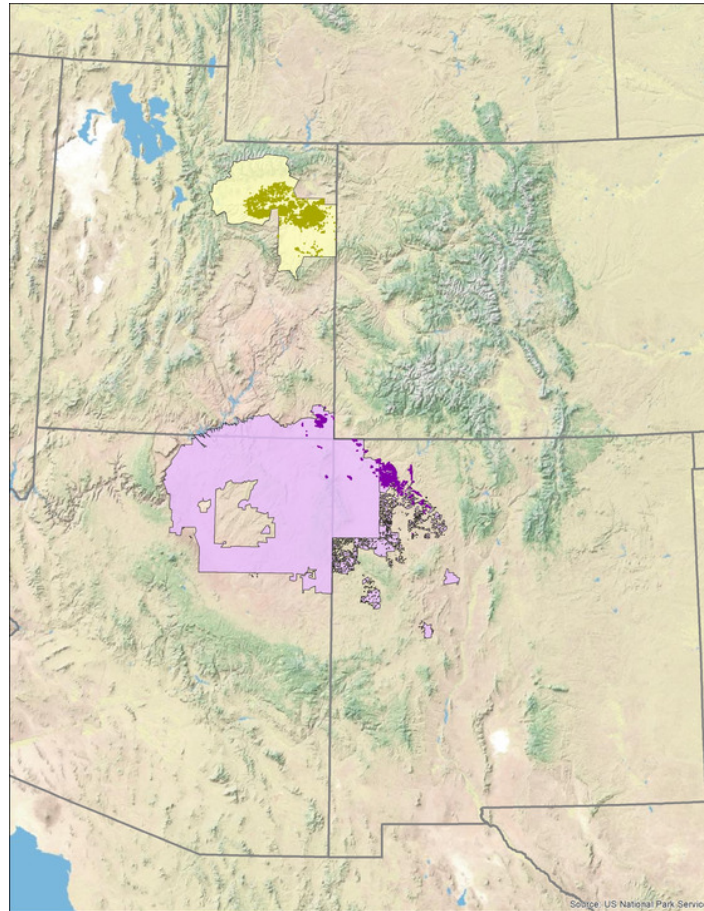


In all of the cases analyzed, tribal communities are more likely to live in the radius than the population as a whole and therefore are disproportionately impacted by oil and gas pollution:

Fort Berthold Indian Reservation	Percent of Population in ½ Mile Radius	Percent of Population Below Poverty Line
Native American Population on Tribal Land	4%	28%
Total State Population — North Dakota	2%	11%



Navajo Nation (Utah and New Mexico only)	Percent of Population in ½ Mile Radius	Percent of Population Below Poverty Line
Native American Population on Tribal Land	7%	42%
Total State Population — Utah and New Mexico	3%	15%



Uintah-Ouray (Northern Ute)	Percent of Population in ½ Mile Radius	Percent of Population Below Poverty Line
Native American Population on Tribal Land	23%	28%
Total State Population — Utah	0.5%	12%

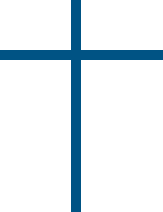
Source:
 Radius data: U.S. Census, 2010. Oil and gas facility data: see <http://oilandgasthreatmap.com/about/data/>.
 Poverty data: American Community Survey, 2016.



Individuals living below the poverty line or without health insurance are particularly burdened by the effects of air pollution. High poverty rates restrict housing options for families, and lack of health insurance limits access to quality health care. These economic factors exacerbate the impact air pollution has on low-income families. [Studies](#) have found that children with asthma that also live in poverty or without insurance are more likely to end up in the emergency room because of asthma attacks, because poverty and lack of quality health insurance can make it hard to keep asthma under control, resulting in more severe attacks and visits to the hospital. Thus, even for the same health risk, the health burden is greater for people living in poverty. Native American individuals living on these tribal lands are more likely to be living in poverty compared to the population of the encompassing state(s).

“Air pollution from the oil and gas industry threatens the health of the Navajo Nation, particularly our children. You can actually smell the gas from some wells while realizing that you can’t have gas service for your house in the winter. Oil and gas companies get rich while members of my community suffer from asthma attacks and nose bleeds and stay poor.”

-Carol Davis, Coordinator Diné Citizens Against Ruining our Environment



The bottom line: air pollution from the oil and gas industry affects Native American communities on tribal lands. Tribal communities need strong safeguards to limit methane, toxic air pollution, and other pollutants that form ozone smog from the oil and gas industry and keep communities healthy.